Published for SISSA by Springer

Received: July 3, 2020
Accepted: October 1, 2020
Published: November 18, 2020

Leptoquarks in oblique corrections and Higgs signal strength: status and prospects

Andreas Crivellin,[a,b] **Dario Müller**[a,b] **and Francesco Saturnino**[c]

[a] *Physik-Institut, Universität Zürich, Winterthurerstrasse 190, CH-8057 Zürich, Switzerland*

[b] *Paul Scherrer Institut, Forschungsstrasse 111, CH-5232 Villigen PSI, Switzerland*

[c] *Albert Einstein Center for Fundamental Physics, Institute for Theoretical Physics, University of Bern, Sidlerstrasse 5, CH-3012 Bern, Switzerland*

E-mail: andreas.crivellin@cern.ch, dario.mueller@psi.ch, saturnino@itp.unibe.ch

Abstract: Leptoquarks (LQs) are predicted within Grand Unified Theories and are well motivated by the current flavor anomalies. In this article we investigate the impact of scalar LQs on Higgs decays and oblique corrections as complementary observables in the search for them. Taking into account all five LQ representations under the Standard Model gauge group and including the most general mixing among them, we calculate the effects in $h \to \gamma\gamma$, $h \to gg$, $h \to Z\gamma$ and the Peskin-Takeuchi parameters S, T and U. We find that these observables depend on the same Lagrangian parameters, leading to interesting correlations among them. While the current experimental bounds only yield weak constraints on the model, these correlations can be used to distinguish different LQ representations at future colliders (ILC, CLIC, FCC-ee and FCC-hh), whose discovery potential we are going to discuss.

Keywords: Beyond Standard Model, Higgs Physics

ArXiv ePrint: 2006.10758

Open Access, © The Authors.
Article funded by SCOAP[3].

https://doi.org/10.1007/JHEP11(2020)094

JHEP11(2020)094

source: https://doi.org/10.48350/151025 | downloaded: 18.4.2024

Contents

JHEP11(2020)094

1 Introduction

Leptoquarks (LQs) are particles which have a specific interaction vertex, connecting a lepton with a quark. They are predicted in Grand Unified Theories [1–4] and were systematically classified in ref. [5] into ten possible representations under the Standard Model (SM) gauge group (five scalar and five vector particles). In recent years, LQs experienced a renaissance due to the emergence of the flavor anomalies. In short, hints for new physics (NP) in $R(D^{(*)})$ [6–11], $b \to s\ell^+\ell^-$ [12–17] and a_μ [18] emerged, with a significance of $> 3\,\sigma$ [19–23], $> 5\sigma$ [24–31] and $> 3\,\sigma$ [32], respectively. It has been shown that LQs can explain $b \to s\ell^+\ell^-$ data [33–57], $R(D^{(*)})$ [33, 34, 36–40, 42–44, 46, 47, 51–53, 55–90] and/or a_μ [55, 56, 62, 71, 74, 77, 86, 91–107].

This strong motivation for LQs makes it also interesting to search for their signatures in other observables. Complementary to direct LHC searches [108–121], oblique electroweak (EW) parameters (S and T parameters [122, 123]) and the corrections to (effective on-shell) couplings of the SM Higgs to photons ($h\gamma\gamma$), Z and photon ($hZ\gamma$) and gluons (hgg) allow to test LQ interactions with the Higgs, independently of the LQ couplings to fermions. In this context, LQs were briefly discussed in ref. [124] based on analogous MSSM calculations [125–127], simplified model analysis [128–131], vacuum stability [132], LQ production at hadron colliders [133] and Higgs pair production [134]. In addition, ref. [135] recently studied LQs in Higgs production and ref. [136] considered $h \to \gamma\gamma$, while ref. [137] performed the matching in the singlet-triplet model [86]. However, none of these analyses

	Φ_1	$\tilde{\Phi}_1$	Φ_2	$\tilde{\Phi}_2$	Φ_3
$\mathcal{G}_{\rm SM}$	$\left(3,1,-\frac{2}{3}\right)$	$\left(3,1,-\frac{8}{3}\right)$	$\left(3,2,\frac{7}{3}\right)$	$\left(3,2,\frac{1}{3}\right)$	$\left(3,3,-\frac{2}{3}\right)$

Table 1. LQ representations under the SM gauge group.

considered more than a single LQ representation at a time. The situation is similar concerning the S and T parameter. This was also briefly discussed in ref. [124], based on simplified model calculations [138] and an analysis discussing only the $SU(2)_L$ doublet LQs [139]. Most importantly, the unavoidable correlations between Higgs couplings to gauge bosons and the oblique parameters were not considered so far. Importantly, these observables can be measured much more precisely at future colliders such as the ILC [140], CLIC [141], and the FCC [142, 143]. Therefore, it is interesting to examine their estimated constraining power and discovery potential.

In this article we will calculate the one-loop effects of LQs in oblique corrections, $h\gamma\gamma$, $hZ\gamma$ and hgg, taking into account all five scalar LQ representations and the complete set of their interactions with the Higgs. In the next section we will define our setup and conventions before we turn to the calculation of the S and T parameters in section 3 and to $h\gamma\gamma$, $hZ\gamma$ and hgg in section 4. We then perform our phenomenological analysis, examining the current status and future prospects for these observables in section 5, before we conclude in section 6. An appendix provides useful analytic (perturbative) expressions for LQ couplings and results for the loop functions.

2 Setup and conventions

There are ten possible representations of LQs under the SM gauge group [5]. While for vector LQs a Higgs mechanism is necessary to render the model renormalizable, scalar LQs can simply be added to the SM. Since we are interested in loop effects in this work, we will focus on the latter ones in the following.

The five different scalar LQs transform under the SM gauge group

$$\mathcal{G}_{\rm SM} = SU(3)_c \times SU(2)_L \times U(1)_Y \tag{2.1}$$

as given in table 1.

We defined the hypercharge Y such that the electromagnetic charge is given by

$$Q = \frac{1}{2} Y + T_3 \,, \tag{2.2}$$

with T_3 representing the third component of weak isospin, e.g. $\pm 1/2$ for $SU(2)_L$ doublets and $1, 0, -1$ for the $SU(2)_L$ triplet. Therefore, we have the following eigenstates with respect to the electric charge

$$\begin{aligned} &\Phi_1 \equiv \Phi_1^{-1/3} \,, \qquad \tilde{\Phi}_1 \equiv \tilde{\Phi}_1^{-4/3} \,, \\ &\Phi_2 \equiv \begin{pmatrix} \Phi_2^{5/3} \\ \Phi_2^{2/3} \end{pmatrix} , \quad \tilde{\Phi}_2 \equiv \begin{pmatrix} \tilde{\Phi}_2^{2/3} \\ \tilde{\Phi}_2^{-1/3} \end{pmatrix} , \quad \tau \cdot \Phi_3 \equiv \begin{pmatrix} \Phi_3^{-1/3} & \sqrt{2}\Phi_3^{2/3} \\ \sqrt{2}\Phi_3^{-4/3} & -\Phi_3^{-1/3} \end{pmatrix} , \end{aligned} \tag{2.3}$$

JHEP11(2020)094

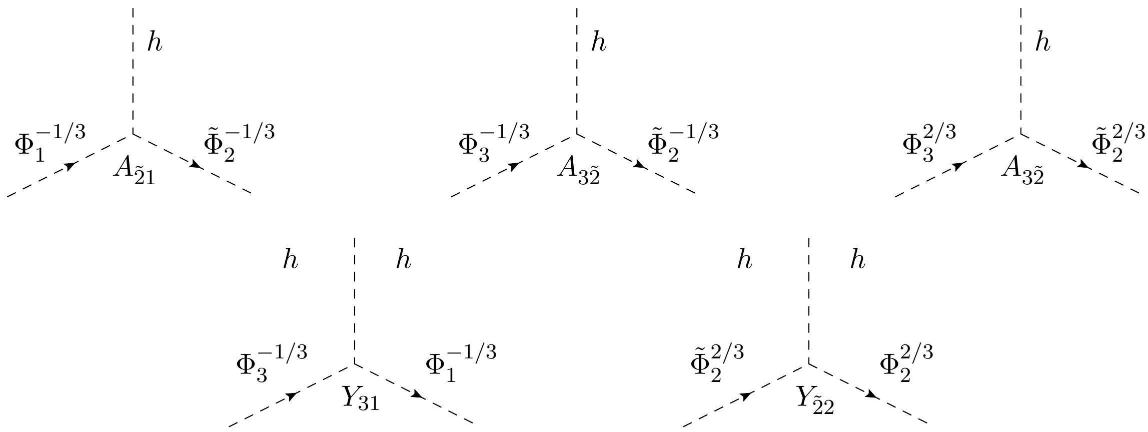

Figure 1. Feynman diagrams depicting LQ-Higgs interactions. Here the physical Higgs h can be replaced by its vev, leading to mixing among the LQs.

obtained from the five representations. Note that the upper index refers to the electric charge and the lower one to the $\mathrm{SU}(2)_L$ representation from which the field originates.

In addition to the gauge interactions of the LQs, determined by the respective representation under the SM gauge group, LQs can couple to the SM Higgs doublet H (with hypercharge +1) via the Lagrangian [144][1]

$$\begin{aligned}
\mathcal{L}_{H\Phi} = & -A_{\tilde{2}1}(\tilde{\Phi}_2^\dagger H)\Phi_1 + A_{3\tilde{2}}(\tilde{\Phi}_2^\dagger(\tau\cdot\Phi_3)H) + Y_{\tilde{2}2}(\Phi_2^\dagger H)(Hi\tau_2\tilde{\Phi}_2) \\
& + Y_{3\tilde{1}}(Hi\tau_2(\tau\cdot\Phi_3)^\dagger H)\tilde{\Phi}_1 + Y_{31}(H^\dagger(\tau\cdot\Phi_3)H)\Phi_1^\dagger + \text{h.c.} \\
& - Y_{22}(Hi\tau_2\Phi_2)(Hi\tau_2\Phi_2)^\dagger - Y_{\tilde{2}\tilde{2}}(Hi\tau_2\tilde{\Phi}_2)(Hi\tau_2\tilde{\Phi}_2)^\dagger \\
& - iY_{33}\varepsilon_{IJK}H^\dagger\tau_I H\Phi_{3,K}^\dagger\Phi_{3,J} \\
& - \sum_{k=1}^{3}(m_k^2 + Y_k H^\dagger H)\Phi_k^\dagger\Phi_k - \sum_{k=1}^{2}(\tilde{m}_k^2 + Y_{\tilde{k}}H^\dagger H)\tilde{\Phi}_k^\dagger\tilde{\Phi}_k\,.
\end{aligned} \tag{2.4}$$

Here m_Φ^2 represent the usual (bare) mass terms of the LQs, present without EW symmetry breaking and ε_{IJK} is the three-dimensional Levi-Civita tensor with $\varepsilon_{123}=1$. Note that $A_{\tilde{2}1}$ and $A_{3\tilde{2}}$ have mass dimension one, while the Y couplings are dimensionless. The LQ-Higgs interactions lead to additional contributions to the mass matrices. The mixing among them is depicted in figure 1.

[1] $Y_{\tilde{2}\tilde{2}}$ and Y_{22} were studied in ref. [139] while the Y_{33} term was considered in ref. [145].

JHEP11(2020)094

Once the Higgs acquires a vacuum expectation value (vev) with $v \approx 174\,\text{GeV}$, this generates the following mass matrices in the interaction basis

$$
\begin{aligned}
\mathcal{M}^{-1/3} &= \begin{pmatrix} m_1^2 + v^2 Y_1 & v A_{\tilde{2}1}^* & v^2 Y_{31} \\ v A_{\tilde{2}1} & \tilde{m}_2^2 + v^2 Y_{\tilde{2}} & v A_{3\tilde{2}} \\ v^2 Y_{31}^* & v A_{3\tilde{2}}^* & m_3^2 + v^2 Y_3 \end{pmatrix} , \\
\mathcal{M}^{2/3} &= \begin{pmatrix} m_2^2 + v^2 Y_2 & v^2 Y_{\tilde{2}2} & 0 \\ v^2 Y_{\tilde{2}2}^* & \tilde{m}_2^2 + v^2 (Y_{\tilde{2}\tilde{2}} + Y_{\tilde{2}}) & -\sqrt{2} v A_{3\tilde{2}} \\ 0 & -\sqrt{2} v A_{3\tilde{2}}^* & m_3^2 + v^2 (Y_3 + Y_{33}) \end{pmatrix} , \\
\mathcal{M}^{-4/3} &= \begin{pmatrix} \tilde{m}_1^2 + v^2 Y_{\tilde{1}} & \sqrt{2} v^2 Y_{3\tilde{1}}^* \\ \sqrt{2} v^2 Y_{3\tilde{1}} & m_3^2 + v^2 (Y_3 - Y_{33}) \end{pmatrix} , \\
\mathcal{M}^{5/3} &= m_2^2 + v^2 (Y_{22} + Y_2) ,
\end{aligned}
\tag{2.5}
$$

such that

$$
- \Phi_Q^\dagger \mathcal{M}^Q \Phi_Q \subset \mathcal{L}_{H\Phi} . \tag{2.6}
$$

This now parametrizes the mass terms in the Lagrangian, where Q is the electric charge and we defined

$$
\Phi_{-1/3} \equiv \begin{pmatrix} \Phi_1^{-1/3} \\ \tilde{\Phi}_2^{-1/3} \\ \Phi_3^{-1/3} \end{pmatrix} \qquad \Phi_{2/3} \equiv \begin{pmatrix} \Phi_2^{2/3} \\ \tilde{\Phi}_2^{2/3} \\ \Phi_3^{2/3} \end{pmatrix} \qquad \Phi_{-4/3} \equiv \begin{pmatrix} \tilde{\Phi}_1^{-4/3} \\ \Phi_3^{-4/3} \end{pmatrix} \qquad \Phi_{5/3} \equiv \Phi_2^{5/3} . \tag{2.7}
$$

In order to arrive at the physical basis we need to diagonalize the mass matrices in eq. (2.5). This can be achieved via

$$
\hat{\mathcal{M}}^Q = W^Q \mathcal{M}^Q W^{Q\dagger} \tag{2.8}
$$

with unitary matrices W^Q. Thus, the interaction eigenstates in eq. (2.7) are rotated as

$$
W^Q \Phi_Q \equiv \hat{\Phi}^Q \tag{2.9}
$$

to arrive at the mass eigenstates. The matrices W^Q for $Q = -1/3$ and $Q = 2/3$ too lengthy to be given analytically in full generality, but can of course be computed numerically. However, in order to obtain the explicit dependence on the Lagrangian parameters A and Y, we diagonalize the mass matrices perturbatively up to $\mathcal{O}(v^2)$, which then yields the

JHEP11(2020)094

following expressions

$$
\begin{aligned}
W^{-1/3} &\approx \begin{pmatrix} 1-\frac{v^2|A_{\tilde{2}1}|^2}{2(m_1^2-\tilde{m}_2^2)^2} & \frac{vA^*_{\tilde{2}1}}{m_1^2-\tilde{m}_2^2} & \frac{v^2(Y_{31}(m_1^2-\tilde{m}_2^2)+A^*_{\tilde{2}1}A_{3\tilde{2}})}{(m_1^2-m_3^2)(m_1^2-\tilde{m}_2^2)} \\ \frac{-vA_{\tilde{2}1}}{m_1^2-\tilde{m}_2^2} & 1-\frac{v^2}{2}\left(\frac{|A_{\tilde{2}1}|^2}{(m_1^2-\tilde{m}_2^2)^2}+\frac{|A_{3\tilde{2}}|^2}{(m_3^2-\tilde{m}_2^2)^2}\right) & \frac{-vA_{3\tilde{2}}}{m_3^2-\tilde{m}_2^2} \\ \frac{-v^2(Y^*_{31}(m_3^2-\tilde{m}_2^2)+A_{\tilde{2}1}A^*_{3\tilde{2}})}{(m_1^2-m_3^2)(m_3^2-\tilde{m}_2^2)} & \frac{vA^*_{3\tilde{2}}}{m_3^2-\tilde{m}_2^2} & 1-\frac{v^2|A_{3\tilde{2}}|^2}{2(m_3^2-\tilde{m}_2^2)^2} \end{pmatrix}, \\
W^{2/3} &\approx \begin{pmatrix} 1 & \frac{v^2Y_{\tilde{2}2}}{m_2^2-\tilde{m}_2^2} & 0 \\ \frac{-v^2Y^*_{\tilde{2}2}}{m_2^2-\tilde{m}_2^2} & 1-\frac{v^2|A_{3\tilde{2}}|^2}{(m_3^2-\tilde{m}_2^2)^2} & \frac{-\sqrt{2}vA_{3\tilde{2}}}{\tilde{m}_2^2-m_3^2} \\ 0 & \frac{\sqrt{2}vA^*_{3\tilde{2}}}{\tilde{m}_2^2-m_3^2} & 1-\frac{v^2|A_{3\tilde{2}}|^2}{(m_3^2-\tilde{m}_2^2)^2} \end{pmatrix}, \qquad (2.10) \\
W^{-4/3} &\approx \begin{pmatrix} 1 & \frac{\sqrt{2}v^2Y^*_{3\tilde{1}}}{\tilde{m}_1^2-m_3^2} \\ \frac{-\sqrt{2}v^2Y_{3\tilde{1}}}{\tilde{m}_1^2-m_3^2} & 1 \end{pmatrix}.
\end{aligned}
$$

The physical LQ masses then read

$$
\begin{aligned}
\left(M_a^{-1/3}\right)^2 &\approx \Bigg(m_1^2+v^2\left(Y_1-\frac{|A_{\tilde{2}1}|^2}{\tilde{m}_2^2-m_1^2}\right),\ \tilde{m}_2^2+v^2\left(Y_{\tilde{2}}+\frac{|A_{\tilde{2}1}|^2}{\tilde{m}_2^2-m_1^2}+\frac{|A_{3\tilde{2}}|^2}{\tilde{m}_2^2-m_3^2}\right), \\
&\qquad m_3^2+v^2\left(Y_3-\frac{|A_{3\tilde{2}}|^2}{\tilde{m}_2^2-m_3^2}\right)\Bigg)_a, \\
\left(M_a^{2/3}\right)^2 &\approx \Bigg(m_2^2+v^2Y_2,\ \tilde{m}_2^2+v^2\left(Y_{\tilde{2}\tilde{2}}+Y_{\tilde{2}}+\frac{2|A_{3\tilde{2}}|^2}{\tilde{m}_2^2-m_3^2}\right), \qquad (2.11) \\
&\qquad m_3^2+v^2\left(Y_3+Y_{33}-\frac{2|A_{3\tilde{2}}|^2}{\tilde{m}_2^2-m_3^2}\right)\Bigg)_a, \\
\left(M_a^{-4/3}\right)^2 &\approx \left(\tilde{m}_1^2+v^2Y_{\tilde{1}},\ m_3^2+v^2(Y_3-Y_{33})\right)_a, \\
\left(M^{5/3}\right)^2 &\approx m_2^2+v^2\left(Y_{22}+Y_2\right),
\end{aligned}
$$

valid up to order v^2, where a runs from 1 to 3 for $Q=-1/3$ and $Q=2/3$ and from 1 to 2 for $Q=-4/3$, respectively.[2]

We now write the interaction terms of the Higgs with the LQs in the form

$$
\begin{aligned}
\mathcal{L}_{H\Phi} = &-\tilde{\Gamma}^{-1/3}_{ab}h\hat{\Phi}^{-1/3\,\dagger}_a\hat{\Phi}^{-1/3}_b-\tilde{\Gamma}^{2/3}_{ab}h\hat{\Phi}^{2/3\,\dagger}_a\hat{\Phi}^{2/3}_b-\tilde{\Gamma}^{-4/3}_{ab}h\hat{\Phi}^{-4/3\dagger}_a\hat{\Phi}^{-4/3}_b \\
&-\Gamma^{5/3}h\hat{\Phi}^{5/3\,\dagger}\hat{\Phi}^{5/3}-\tilde{\Lambda}^{-1/3}_{ab}h^2\hat{\Phi}^{-1/3\,\dagger}_a\hat{\Phi}^{-1/3}_b-\tilde{\Lambda}^{2/3}_{ab}h^2\hat{\Phi}^{2/3\,\dagger}_a\hat{\Phi}^{2/3}_b \qquad (2.12) \\
&-\tilde{\Lambda}^{-4/3}_{ab}h^2\hat{\Phi}^{-4/3\,\dagger}_a\hat{\Phi}^{-4/3}_b-\Lambda^{5/3}h^2\hat{\Phi}^{5/3\,\dagger}\hat{\Phi}^{5/3},
\end{aligned}
$$

with h as the physical Higgs field, $\hat{\Phi}^Q$ being the mass eigenstates of charge Q with a,b again running from 1 to 3 for $Q=-1/3$ and $Q=2/3$ and from 1 to 2 for $Q=-4/3$. In

[2]For the calculation of the T parameter, we even needed the expansion of the mixing matrices and masses up to order v^4. However, these equations are too lengthy to be included in this work explicitly.

JHEP11(2020)094

particular we have

$$
\begin{aligned}
\tilde{\Gamma}^{-1/3} &= W^{-1/3}\Gamma^{-1/3}W^{-1/3\,\dagger}\,, & \tilde{\Lambda}^{1/3} &= W^{-1/3}\Lambda^{-1/3}W^{-1/3\,\dagger}\,,\\
\tilde{\Gamma}^{2/3} &= W^{2/3}\Gamma^{2/3}W^{2/3\,\dagger}\,, & \tilde{\Lambda}^{2/3} &= W^{2/3}\Lambda^{2/3}W^{2/3\,\dagger}\,,\\
\tilde{\Gamma}^{-4/3} &= W^{-4/3}\Gamma^{-4/3}W^{-4/3\,\dagger}\,, & \tilde{\Lambda}^{-4/3} &= W^{-4/3}\Lambda^{-4/3}W^{-4/3\,\dagger}\,,
\end{aligned}
\tag{2.13}
$$

with

$$
\begin{aligned}
\Gamma^{-1/3} &= \frac{1}{\sqrt{2}}\begin{pmatrix} 2vY_1 & A^*_{\tilde{2}1} & 2vY_{31}\\ A_{\tilde{2}1} & 2vY_{\tilde{2}} & A_{3\tilde{2}}\\ 2vY^*_{31} & A^*_{3\tilde{2}} & 2vY_3 \end{pmatrix}, & \Lambda^{-1/3} &= \frac{1}{2}\begin{pmatrix} Y_1 & 0 & Y_{31}\\ 0 & Y_{\tilde{2}} & 0\\ Y^*_{31} & 0 & Y_3 \end{pmatrix},\\
\Gamma^{2/3} &= \frac{1}{\sqrt{2}}\begin{pmatrix} 2vY_2 & 2vY^*_{\tilde{2}2} & 0\\ 2vY_{\tilde{2}2} & 2v(Y_{\tilde{2}}+Y_{\tilde{2}\tilde{2}}) & -\sqrt{2}A^*_{3\tilde{2}}\\ 0 & -\sqrt{2}A_{3\tilde{2}} & 2v(Y_3+Y_{33}) \end{pmatrix}, & \Lambda^{2/3} &= \frac{1}{2}\begin{pmatrix} Y_2 & Y^*_{\tilde{2}2} & 0\\ Y_{\tilde{2}2} & Y_{\tilde{2}}+Y_{\tilde{2}\tilde{2}} & 0\\ 0 & 0 & Y_3+Y_{33} \end{pmatrix},\\
\Gamma^{-4/3} &= \frac{1}{\sqrt{2}}\begin{pmatrix} 2vY_{\tilde{1}} & 2vY^*_{3\tilde{1}}\\ 2vY_{3\tilde{1}} & 2v(Y_3-Y_{33}) \end{pmatrix}, & \Lambda^{-4/3} &= \frac{1}{2}\begin{pmatrix} Y_{\tilde{1}} & Y^*_{3\tilde{1}}\\ Y_{3\tilde{1}} & Y_3-Y_{33} \end{pmatrix}.\\
\Gamma^{5/3} &= \sqrt{2}v(Y_{22}+Y_2)\,, & \Lambda^{5/3} &= \frac{1}{2}(Y_{22}+Y_2)\,.
\end{aligned}
\tag{2.14}
$$

The expanded expressions for $\tilde{\Gamma}^Q$ and $\tilde{\Lambda}^Q$ up to $\mathcal{O}(v^2)$ are given in the appendix.

3 Oblique corrections

Oblique Corrections, i.e. radiative corrections to the EW breaking sector of the SM, can be parametrized via the Peskin-Takeuchi parameters S, T and U [146]. These parameters are expressed and calculated in terms of the vacuum polarization functions $\Pi_{VV}(q^2)$, with $V = W, Z, \gamma$. We use the convention

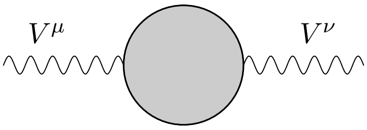

$$
= i\Pi_{VV}(q^2)g^{\mu\nu} - i\Delta(q^2)q^\mu q^\nu\,. \tag{3.1}
$$

Taking into account that our NP scale is higher than the EW breaking scale, we can expand the gauge bosons self-energies in q^2/M^2. As $\Delta(q^2)$ has no physical effect, the three oblique parameters can be written as

$$
\begin{aligned}
S &= -\frac{4s_w^2c_w^2}{\alpha m_Z^2}\left(\Pi_{ZZ}(0) - \Pi_{ZZ}(m_Z^2) + \Pi_{\gamma\gamma}(m_Z^2) + \frac{c_w^2 - s_w^2}{c_w s_w}\Pi_{Z\gamma}(m_Z^2)\right),\\
T &= \frac{\Pi_{WW}(0)}{\alpha m_W^2} - \frac{\Pi_{ZZ}(0)}{\alpha m_Z^2}\,,\\
U &= -\frac{4s_w^2c_w^2}{\alpha}\left(\frac{\Pi_{WW}(0) - \Pi_{WW}(m_W^2)}{c_w^2 m_W^2} - \frac{\Pi_{ZZ}(0) - \Pi_{ZZ}(m_Z^2)}{m_Z^2}\right.\\
&\qquad\left. + \frac{s_w^2}{c_w^2}\frac{\Pi_{\gamma\gamma}(m_Z^2)}{m_Z^2} + 2\frac{s_w}{c_w}\frac{\Pi_{Z\gamma}(m_Z^2)}{m_Z^2}\right),
\end{aligned}
\tag{3.2}
$$

JHEP11(2020)094

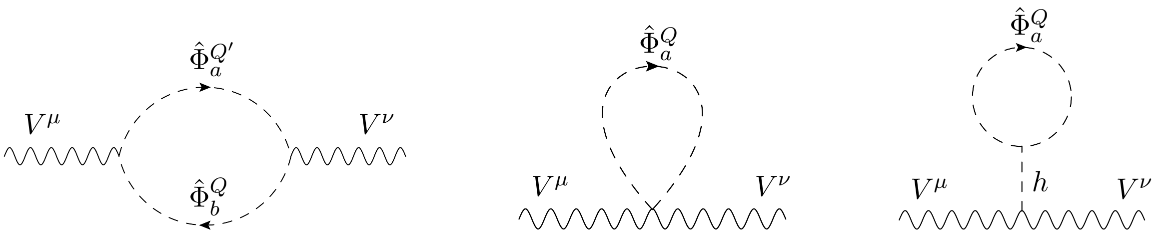

Figure 2. The three different topologies of Feynman diagrams that contribute to $\Pi_{VV}(q^2)$ with $V = W, Z, \gamma$. The last diagram only exists for $V = W, Z$ and has no impact on the S, T and U parameters as it is momentum independent.

where we used renormalization conditions for the vector fields such that

$$\Pi_{\gamma\gamma}(0) = \Pi_{Z\gamma}(0) = \mathrm{Re}[\Pi_{ZZ}(m_Z^2)] = \mathrm{Re}[\Pi_{WW}(m_W^2)] = 0\,. \tag{3.3}$$

These conditions are fulfilled automatically for $\Pi_{\gamma\gamma}$ and $\Pi_{Z\gamma}$ because of the Ward identities.

S, T and U can be calculated with the bare (unrenormalized) two-point correlation functions, the corresponding diagrams in our model are shown in figure 2. Therefore, we used the check that all divergences disappear in the physical observables S, T and U after having summed over all $\mathrm{SU}(2)_L$ components in the loop. The complete expressions for these parameters are quite lengthy and therefore given in the appendix. Expanding in addition in q^2/M^2 and in v/M, i.e. perturbatively diagonalizing the LQ mass matrices, we can however obtain relatively compact expressions. Up to leading order in v we find

$$\begin{aligned}
S \approx& -\frac{N_c v^2}{36\pi}\left(\frac{7Y_{22}}{m_2^2}+\frac{Y_{\tilde{2}\tilde{2}}}{\tilde{m}_2^2}-\frac{8Y_{33}}{m_3^2}-\frac{|A_{\tilde{2}1}|^2}{10\tilde{m}_2^4}\mathcal{K}_1\left(\frac{m_1^2}{\tilde{m}_2^2}\right)+\frac{17|A_{3\tilde{2}}|^2}{10\tilde{m}_2^4}\mathcal{K}_2\left(\frac{m_3^2}{\tilde{m}_2^2}\right)\right),\\
T \approx& \frac{N_c v^2}{24\pi g_2^2 s_w^2}\left(\frac{Y_{22}^2}{m_2^2}+\frac{Y_{\tilde{2}\tilde{2}}^2}{\tilde{m}_2^2}+\frac{4Y_{33}^2}{m_3^2}+\frac{|A_{\tilde{2}1}|^4}{10\tilde{m}_2^6}\mathcal{K}_3\left(\frac{m_1^2}{\tilde{m}_2^2}\right)+\frac{|A_{3\tilde{2}}|^4}{2\tilde{m}_2^6}\mathcal{K}_4\left(\frac{m_3^2}{\tilde{m}_2^2}\right)+\frac{Y_{\tilde{2}\tilde{2}}|A_{\tilde{2}1}|^2}{2\tilde{m}_2^4}\mathcal{K}_5\left(\frac{m_1^2}{\tilde{m}_2^2}\right)\right.\\
&-\frac{Y_{\tilde{2}\tilde{2}}|A_{3\tilde{2}}|^2}{2\tilde{m}_2^4}\mathcal{K}_5\left(\frac{m_3^2}{\tilde{m}_2^2}\right)-2\frac{Y_{33}|A_{3\tilde{2}}|^2}{\tilde{m}_2^4}\mathcal{K}_6\left(\frac{m_3^2}{\tilde{m}_2^2}\right)+\frac{4|Y_{31}|^2}{m_3^2}\mathcal{K}_7\left(\frac{m_1^2}{m_3^2}\right)-\frac{4|Y_{3\tilde{1}}|^2}{m_3^2}\mathcal{K}_7\left(\frac{\tilde{m}_1^2}{m_3^2}\right)\\
&\left.-\frac{2|Y_{2\tilde{2}}|^2}{\tilde{m}_2^2}\mathcal{K}_7\left(\frac{m_2^2}{\tilde{m}_2^2}\right)-\frac{2\Re[Y_{31}A_{\tilde{2}1}A_{3\tilde{2}}^*]}{\tilde{m}_2^4}\mathcal{K}_8\left(\frac{m_1^2}{\tilde{m}_2^2},\frac{m_3^2}{\tilde{m}_2^2}\right)+\frac{|A_{\tilde{2}1}|^2|A_{3\tilde{2}}|^2}{5\tilde{m}_2^6}\mathcal{K}_9\left(\frac{m_1^2}{\tilde{m}_2^2},\frac{m_3^2}{\tilde{m}_2^2}\right)\right),\\
U \approx& \,0\,,
\end{aligned} \tag{3.4}$$

where the loop functions, given in the appendix, are normalized to be unity in case of equal masses. These expressions agree with refs. [138, 139] for the special cases studied there. Note that U is approximately zero since it only arises at dimension 8.

4 Higgs couplings to g, γ and Z

The Feynman diagrams involving scalar LQs contributing to $h \to \gamma\gamma$, $h \to gg$ and $h \to Z\gamma$ are shown in figure 3. The amplitude, induced by them, reads

$$\mathcal{A}[h \to \gamma(p_1)\gamma(p_2)] = \frac{\alpha N_c}{24\pi}\sum_{Q,a}\frac{Q^2\tilde{\Gamma}_{aa}^Q}{\left(M_a^Q\right)^2}\left(m_h^2\varepsilon(p_1)\cdot\varepsilon(p_2) - 2(\varepsilon(p_1)\cdot p_2)(\varepsilon(p_2)\cdot p_1)\right), \tag{4.1}$$

JHEP11(2020)094

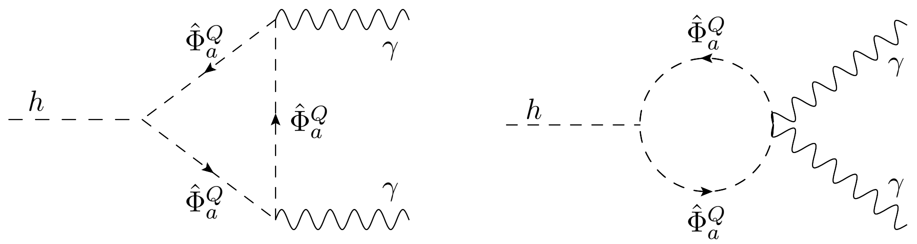

Figure 3. The two types of diagrams that induce NP effects in $h \to \gamma\gamma$. For $h \to gg$ the photons can simply be replaced by gluons, for $h \to Z\gamma$ one photon can be replaced by a Z boson. The additional diagrams with reversed charge flow are not depicted.

with p_1 and p_2 representing the photon momenta, $\varepsilon_\mu(p_i)$ the corresponding polarization vectors and a running over the number of mass eigenstates with the same electric charge $Q = \{-1/3,\ 2/3,\ -4/3,\ 5/3\}$. Here we used on-shell kinematics and expanded in m_h^2/M^2.

Similarly, for the decay into a pair of gluons, we obtain

$$\mathcal{A}[h \to g^A(p_1) g^A(p_2)] = \frac{\alpha_s}{48\pi} \sum_Q \frac{\tilde\Gamma^Q_{aa}}{\left(M_a^Q\right)^2} \left(m_h^2 \varepsilon^A(p_1)\cdot\varepsilon^A(p_2) - 2(\varepsilon^A(p_1)\cdot p_2)(\varepsilon^A(p_2)\cdot p_1)\right),$$

where A labels the 8 gluons (no sum implied). For the Higgs decaying into a Z and a photon we obtain

$$\begin{aligned}\mathcal{A}[h \to Z(p_Z)\gamma(p_\gamma)] = {} & \frac{\alpha N_c}{24\pi} \frac{1}{s_w c_w} \sum_Q \left(Q \frac{\tilde\Gamma^Q_{ab} \tilde\Gamma^Q_{ba}}{\left(M_b^Q\right)^2} \mathcal{K}_7\left(x^Q_{ab}\right) - s_w^2 Q^2 \frac{\tilde\Gamma^Q_{aa}}{\left(M_a^Q\right)^2} \right) \\ & \times \left((m_h^2 - m_Z^2)\, \varepsilon(p_Z)\cdot\varepsilon(p_\gamma) - 2(\varepsilon(p_Z)\cdot p_\gamma)(\varepsilon(p_\gamma)\cdot p_Z) \right),\end{aligned} \tag{4.2}$$

with a simultaneous expansion in m_h^2/M^2 and m_Z^2/M^2 and

$$x^Q_{ab} = \frac{\left(M_a^Q\right)^2}{\left(M_b^Q\right)^2}. \tag{4.3}$$

The relevant observables in this context are the effective on-shell $h\gamma\gamma$, hgg and $hZ\gamma$ couplings, normalized to their SM values

$$\kappa_\gamma = \sqrt{\frac{\Gamma_{h\to\gamma\gamma}}{\Gamma^{\rm SM}_{h\to\gamma\gamma}}}, \qquad \kappa_g = \sqrt{\frac{\Gamma_{h\to gg}}{\Gamma^{\rm SM}_{h\to gg}}}, \qquad \kappa_{Z\gamma} = \sqrt{\frac{\Gamma_{h\to Z\gamma}}{\Gamma^{\rm SM}_{h\to Z\gamma}}}. \tag{4.4}$$

We then have

$$\begin{aligned}\kappa_\gamma &= 1 + \frac{1}{\mathcal{A}^{\rm SM}_{h\to\gamma\gamma}} \frac{\alpha N_c}{24\pi} \sum_Q Q^2 \frac{\tilde\Gamma^Q_{aa}}{\left(M_a^Q\right)^2}, \\ \kappa_g &= 1 + \frac{1}{\mathcal{A}^{\rm SM}_{h\to gg}} \frac{\alpha_s}{48\pi} \sum_Q \frac{\tilde\Gamma^Q_{aa}}{\left(M_a^Q\right)^2}, \\ \kappa_{Z\gamma} &= 1 - \frac{1}{\mathcal{A}^{\rm SM}_{h\to Z\gamma}} \frac{\alpha N_c}{24\pi} \frac{1}{s_w c_w} \sum_Q \left(Q \frac{\tilde\Gamma^Q_{ab} \tilde\Gamma^Q_{ba}}{\left(M_b^Q\right)^2} \mathcal{K}_6\left(x^Q_{ab}\right) - s_w^2 Q^2 \frac{\tilde\Gamma^Q_{aa}}{\left(M_a^Q\right)^2} \right),\end{aligned} \tag{4.5}$$

JHEP11(2020)094

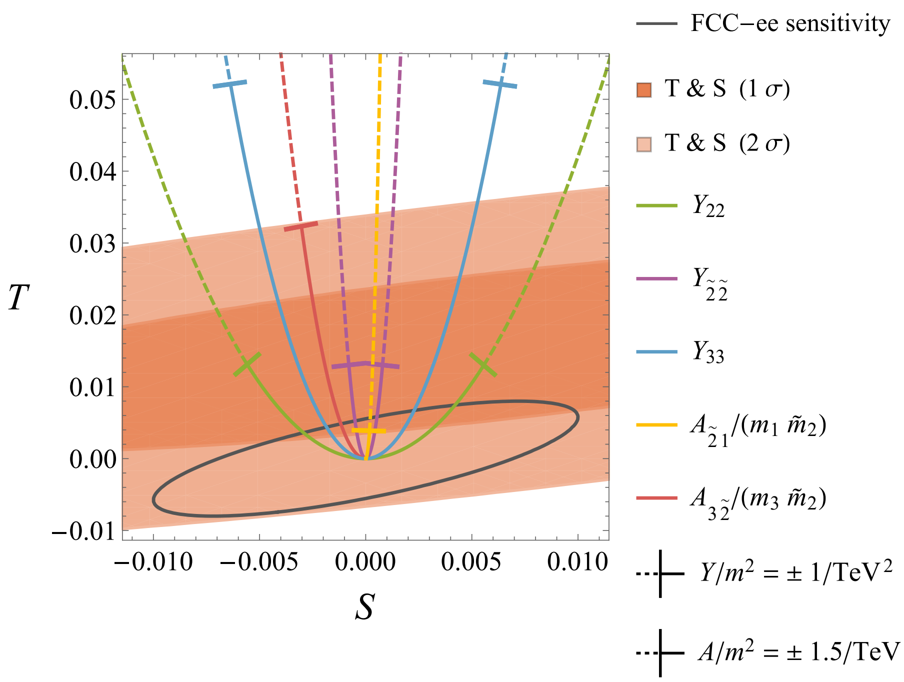

Figure 4. Correlations between S and T for four different Lagrangian parameters in eq. (2.4), assuming that only one of them is non-zero at a time. For simplicity, we assumed all LQ masses to be equal. While Y_{22} and $Y_{\tilde{2}\tilde{2}}$ can yield both positive and negative effects in S, the effect in the T parameter is positive definite. Since our prediction for S and T depends on a single combination of parameters (Y/m^2 or A^2/m^4), we used one degree of freedom to obtain the preferred region in the S-T plane, such that the region within the ellipse labelled by $1\,\sigma$ ($2\,\sigma$) corresponds to 68% C.L. (95% C.L.).

with the LO SM amplitudes (see e.g. ref. [147] for an overview) given by [124, 148–153]

$$
\begin{aligned}
\mathcal{A}^{\text{SM}}_{h\to\gamma\gamma} &= \frac{\alpha}{4\pi\sqrt{2}v}\left(A_1(x_W) + \frac{4}{3}A_{1/2}(x_t)\right),\\
\mathcal{A}^{\text{SM}}_{h\to gg} &= \frac{\alpha_s}{8\pi\sqrt{2}v}A_{1/2}(x_t)\,,\\
\mathcal{A}^{\text{SM}}_{h\to Z\gamma} &= \frac{\alpha}{4\pi s_w\sqrt{2}v}\left(c_w C_1(x_W^{-1}, y_W) + \frac{2}{c_w}\left(1-\frac{8}{3}s_w^2\right)C_{1/2}(x_t^{-1}, y_t)\right).
\end{aligned}
\tag{4.6}
$$

We defined

$$
x_i = \frac{m_h^2}{4m_i^2}\,, \qquad y_i = \frac{4m_i^2}{m_Z^2}\,, \tag{4.7}
$$

while the loop functions are given in the appendix.[3]

[3]Note that we did not include the effects of bottom quarks in the SM prediction which would lead to a 10% destructive interference.

JHEP11(2020)094

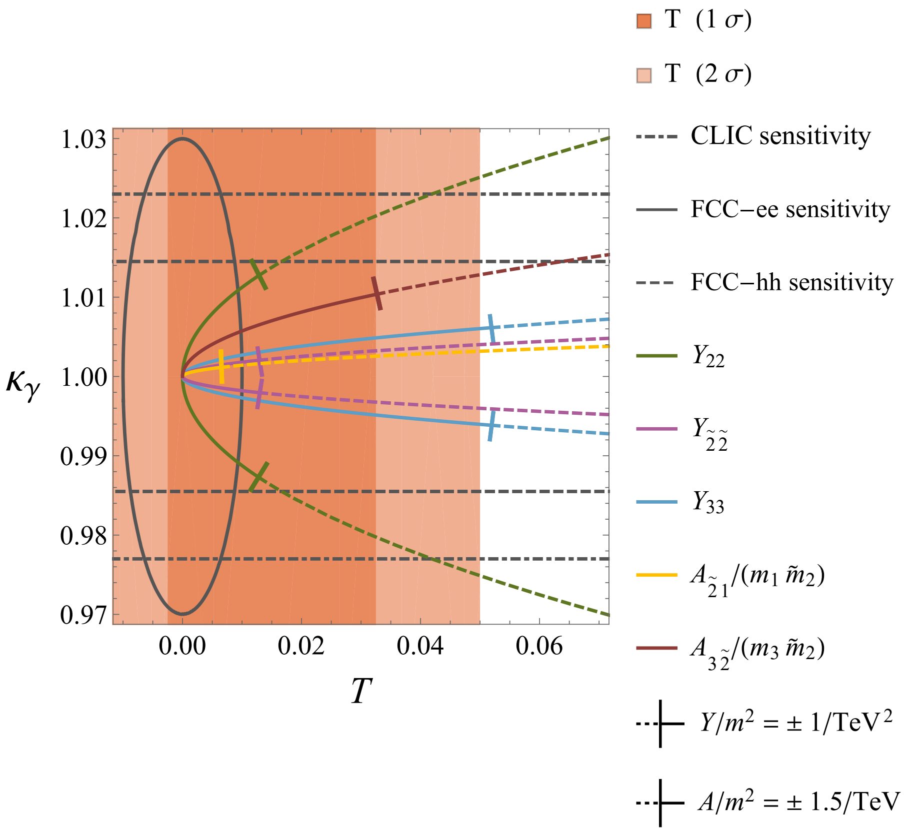

Figure 5. Correlations between κ_γ and T for different Lagrangian parameters, assuming that only one of them is non-zero at a time and assuming all LQ masses to be equal.

In addition to the expansion of the loop functions, we can also expand the expressions $\tilde{\Gamma}^Q/M^2$ and $\tilde{T}^Q\,\tilde{\Gamma}^Q\,\mathcal{K}_6(x^Q_{ab})/M^2$ in v^2/M^2 up to $\mathcal{O}(v^3)$, using eq. (2.10). We obtain

$$
\begin{aligned}
\sum_{a=1}^{3}\frac{\tilde{\Gamma}^{-1/3}_{aa}}{\left(M_a^{-1/3}\right)^2} &\approx \sqrt{2}v\left(\frac{Y_1}{m_1^2}+\frac{Y_{\tilde{2}}}{\tilde{m}_2^2}+\frac{Y_3}{m_3^2}-\frac{|A_{\tilde{2}1}|^2}{m_1^2\tilde{m}_2^2}-\frac{|A_{3\tilde{2}}|^2}{m_3^2\tilde{m}_2^2}\right),\\
\sum_{a=1}^{3}\frac{\tilde{\Gamma}^{2/3}_{aa}}{\left(M_a^{2/3}\right)^2} &\approx \sqrt{2}v\left(\frac{Y_2}{m_2^2}+\frac{Y_{\tilde{2}\tilde{2}}+Y_{\tilde{2}}}{\tilde{m}_2^2}+\frac{Y_3+Y_{33}}{m_3^2}-\frac{2|A_{3\tilde{2}}|^2}{\tilde{m}_2^2m_3^2}\right),\\
\sum_{a=1}^{2}\frac{\tilde{\Gamma}^{-4/3}_{aa}}{\left(M_a^{-4/3}\right)^2} &\approx \sqrt{2}v\left(\frac{Y_{\tilde{1}}}{\tilde{m}_1^2}+\frac{Y_3-Y_{33}}{m_3^2}\right),\\
\frac{\Gamma^{5/3}}{\left(M^{5/3}\right)^2} &\approx \sqrt{2}v\frac{Y_{22}+Y_2}{m_2^2}, \qquad (4.8)\\
\sum_{a,b=1}^{3}\frac{\tilde{T}^{-1/3}_{ab}\,\tilde{\Gamma}^{-1/3}_{ba}}{\left(M_b^{-1/3}\right)^2}\,\mathcal{K}_7(x_{ab}^{-1/3}) &\approx \frac{v}{\sqrt{2}}\left(\frac{|A_{21}|^2}{2\tilde{m}_2^4}\mathcal{F}_1\left(\frac{m_1^2}{\tilde{m}_2^2}\right)+\frac{|A_{32}|^2}{2\tilde{m}_2^4}\mathcal{F}_1\left(\frac{m_3^2}{\tilde{m}_2^2}\right)-\frac{Y_{\tilde{2}}}{\tilde{m}_2^2}\right),\\
\sum_{a,b=1}^{3}\frac{\tilde{T}^{2/3}_{ab}\,\tilde{\Gamma}^{2/3}_{ba}}{\left(M_b^{2/3}\right)^2}\,\mathcal{K}_7(x_{ab}^{2/3}) &\approx \frac{v}{\sqrt{2}}\left(\frac{Y_{\tilde{2}}}{\tilde{m}_2^2}-\frac{Y_2}{m_2^2}+\frac{2(Y_3+Y_{33})}{m_3^2}+\frac{Y_{\tilde{2}\tilde{2}}}{\tilde{m}_2^2}-\frac{3|A_{32}|^2}{\tilde{m}_2^4}\mathcal{F}_2\left(\frac{m_3^2}{\tilde{m}_2^2}\right)\right),
\end{aligned}
$$

JHEP11(2020)094

$$
\begin{aligned}
\sum_{a,b=1}^{2} \frac{\tilde{T}_{ab}^{-4/3}\,\tilde{\Gamma}_{ba}^{-4/3}}{\left(M_b^{-4/3}\right)^2}\,\mathcal{K}_7\!\left(x_{ab}^{-4/3}\right) &\approx -\sqrt{2}v\frac{Y_3 - Y_{33}}{m_3^2}\,,\\
\frac{\tilde{T}^{5/3}\,\tilde{\Gamma}^{5/3}}{\left(M^{5/3}\right)^2} &\approx \frac{v}{\sqrt{2}}\frac{Y_{22}+Y_2}{m_2^2}\,.
\end{aligned}
\tag{4.9}
$$

Therefore, we have directly expressed κ_γ, κ_g and $\kappa_{Z\gamma}$ in terms of the Lagrangian parameters. The loop functions $\mathcal{F}_1$ and $\mathcal{F}_2$, given in the appendix, are again normalized to be unity in case of equal masses.

5 Phenomenological analysis

Before we illustrate the effects of LQs in the observables of our interest, let us recall the current experimental situation and the prospects at future colliders. Concerning the oblique corrections, the global fit to electroweak precision measurements (including LEP [154], Tevatron [155] and LHC [156]) of ref. [157] constrains the S and T parameter to lie within

(5.1)

at 95% C.L. within the 2-dimensional S-T plane, with a correlation factor of 0.72. Here, we can optimistically expect a sensitivity of 0.008 in the future at the FCC-ee [143].

For on-shell Higgs couplings, we used the results of refs. [158, 159] for the current status, which are

$$
\kappa_g = 1.066^{+0.051}_{-0.050}\,, \qquad\qquad \kappa_\gamma = 0.999^{+0.055}_{-0.053}\,. \tag{5.2}
$$

Concerning future prospects we expect for κ_γ (κ_g) an accuracy of 7% (2.3%) at the ILC [140], 3.7% (1.5%) at CEPC [160], 2.3% (0.9%) at CLIC [141], 3% (1.4%) at the FCC-ee [143] and 1.45% at the FCC-hh [161]. Finally, concerning $h \to Z\gamma$, an accuracy of up to 1.8% in $h \to Z\mu^+\mu^-/h \to \mu^+\mu^-$ can be achieved at the FCC-ee [143].

Let us start by considering the oblique parameters. Here and in the following, we will for definiteness assume a LQ mass of 1 TeV, which is compatible with current LHC limits [162–164] for a broad range of couplings to fermions. In figure 4 we show the correlations between S and T for the four cases which contribute to both parameters simultaneously. As one can see, the effect in T is positive definite, as slightly preferred by current data. Note that the A parameters are dimensionful couplings which are naturally expected to be of the same order as the LQ masses and that similarly the dimensionless couplings Y are expected to be of order 1. Therefore, T already now sets relevant limits on these couplings and its future experimental sensitivity allows for stringent constraints or even to discover deviations from the SM within LQ models.

Turning to the effects in Higgs couplings to gauge bosons, we show the correlations between κ_γ and T in figure 5 and between κ_γ and κ_g in figure 6. The currently allowed regions (1 σ and 2 σ, corresponding to 68% and 95% C.L. for one degree of freedom) are shown in color while the future prospects are indicated by dashed and dotted boundaries of the corresponding ellipses. Assuming a value close to the current best fit point in the

JHEP11(2020)094

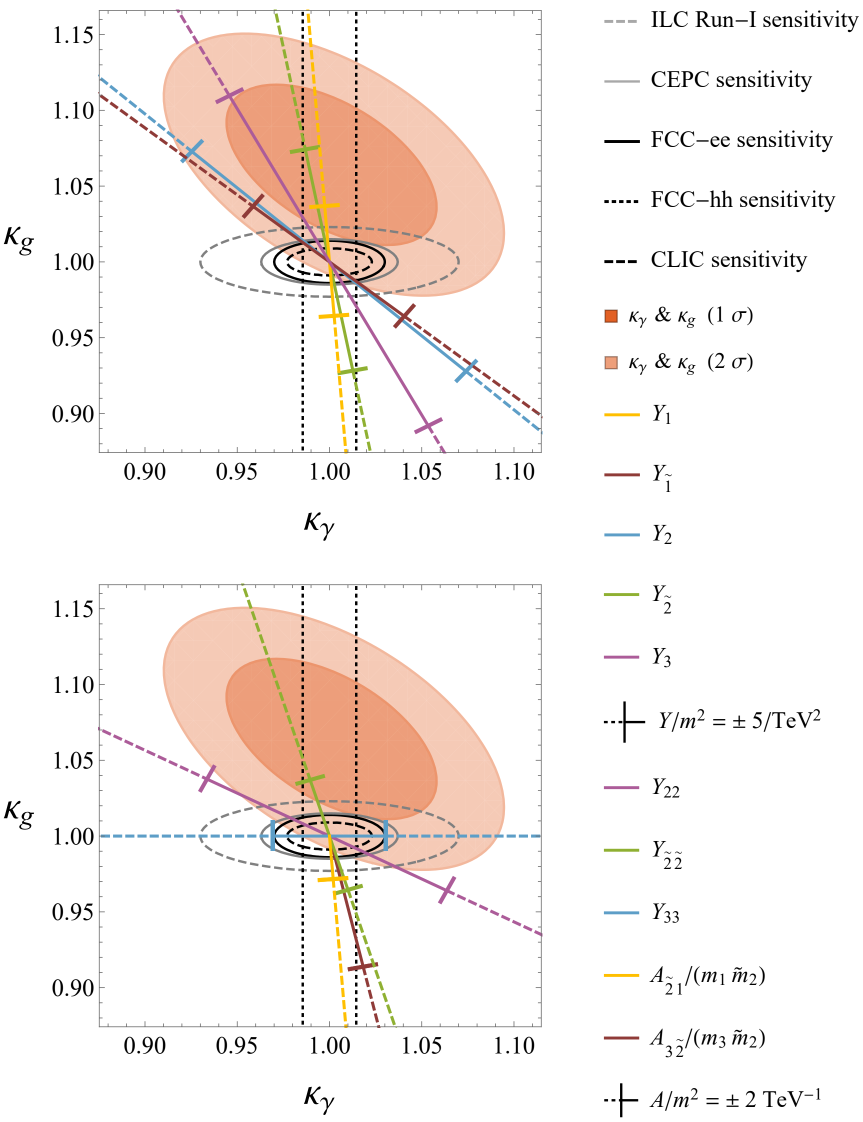

Figure 6. Correlations between κ_γ and κ_g for the different Lagrangian parameters. Here we assumed all bi-linear LQ mass terms to be equal. Here we used one degree of freedom in the χ^2 fit for the allowed regions and the future prospects such that the intersection with the LQ line indicates the 68% and 95% CL for the corresponding parameter Y/m^2 or A^2/m^4.

JHEP11(2020)094

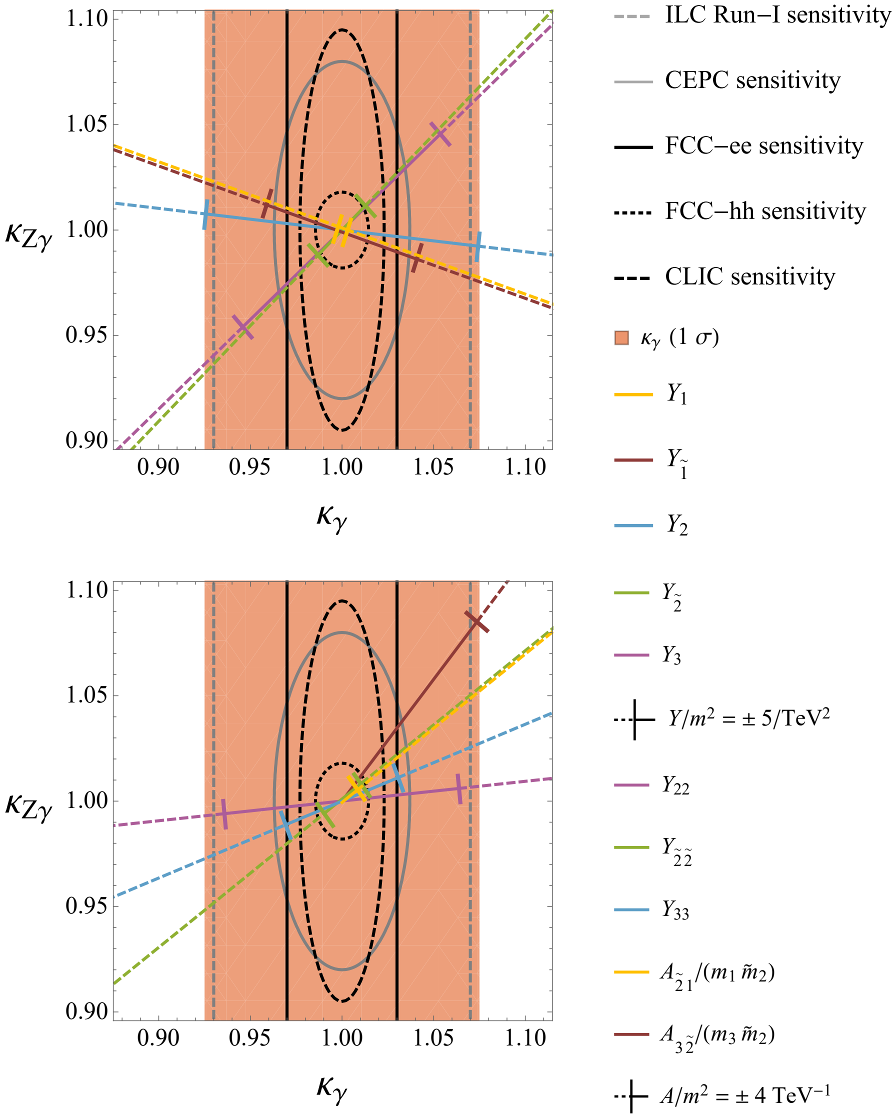

Figure 7. Correlations between κ_γ and $\kappa_{Z\gamma}$ for the different Lagrangian parameters coupling LQs to the Higgs. The currently preferred regions are shown as red ellipses and the future sensitivity is indicated by the dashed and dotted lines.

κ_γ-κ_g plane is confirmed in the future, this would point towards the LQ representation $\tilde{\Phi}_2$. Similarly, one can correlate κ_γ to $\kappa_{Z\gamma}$, see figure 7, which clearly provides complementary distinguishing power, especially at the FCC-hh. E.g. an anti-correlations between κ_γ to $\kappa_{Z\gamma}$ is not favored by either (single) Lagrangian parameter of coupling LQs to the Higgs.

JHEP11(2020)094

6 Conclusions

LQs are prime candidates to explain the flavor anomalies, i.e. the discrepancies between the SM predictions and experiment in $b \to c\tau\nu$ and $b \to s\ell^+\ell^-$ processes and in the anomalous magnetic moment of the muon. Therefore, it is interesting to study alternative observables which are sensitive to LQs and could therefore as well show deviations from the SM predictions. In this context, parameters sensitive to additional electroweak symmetry breaking effects provide a complementary window. In particular, LQ couplings to the SM Higgs generate loop effects, which contribute to the oblique parameters (S and T) and to effective Higgs couplings, entering on-shell Higgs boson production ($gg \to h$) and decays ($h \to \gamma\gamma$, $h \to Z\gamma$). All these observables have in common that (at the one-loop level) they do not depend on the LQ couplings to fermions but rather only on LQ couplings to Higgses (tri-linear and quadratic ones). Therefore, one can test this sector of the Lagrangian independently of the fermion couplings entering flavor observables.

Taking into account the most general set of Higgs-LQ interactions, including mixing among different LQ representations, we calculated the one-loop contributions to the oblique parameters S, T and U. Using a perturbative expansion of the mixing matrices we were able to provide simple, analytic expressions for them. Similarly, we calculated the contributions to effective on-shell hgg, $h\gamma\gamma$ and $hZ\gamma$ couplings, expressing the corrections as simple analytic functions of the Lagrangian parameters.

In our phenomenological analysis we correlated the effects in the oblique corrections with each other, see figure 4, finding that the contribution to T is positive definite and that T is clearly more sensitive to LQs than S. Similarly, we correlated hgg with $h\gamma\gamma$ in figure 6 and $h\gamma\gamma$ to $hZ\gamma$ in figure 7. In the future it would be very interesting to include the NLO QCD corrections, in the spirit of refs. [126, 127], as these interesting correlations open the possibility of distinguishing different LQ representations, independently of their couplings to fermions, providing strong motivation for future colliders.

Acknowledgments

We thank Michael Spira for useful discussions. The work of A.C. and D.M. is supported by a Professorship Grant (PP00P2_176884) of the Swiss National Science Foundation. The work of F.S. is supported by the Swiss National Foundation grant 200020_175449/1.

A Loop functions, exact results and perturbative diagonalization

A.1 Loop functions

In this appendix we first present the loop functions, which are used in (3.4) to write the results for the S and T parameters in a compact form

$$\mathcal{K}_1(y) = -10\left(\frac{y^3+2y^2-19y+4}{(y-1)^4} - \frac{(4y^3-12y^2-6y+2)\log(y)}{(y-1)^5}\right),$$
$$\mathcal{K}_2(y) = \frac{10}{17}\left(\frac{-y^4+10y^3-45y^2-8y+8}{y(y-1)^4} + \frac{18(3y-1)\log(y)}{(y-1)^5}\right),$$

JHEP11(2020)094

$$\mathcal{K}_3(y) = 10\Big(\frac{y^2+10y+1}{(y-1)^4} - \frac{6y(y+1)\log(y)}{(y-1)^5}\Big)\,,$$

$$\mathcal{K}_4(y) = 2\Big(\frac{(y+4)(y^2+10y+1)}{y(y-1)^4} - \frac{6(y+1)(y+4)\log(y)}{(y-1)^5}\Big)\,,$$

$$\mathcal{K}_5(y) = 2\Big(\frac{2y^2+5y-1}{(y-1)^3} - \frac{6y^2\log(y)}{(y-1)^4}\Big)\,,$$

$$\mathcal{K}_6(y) = 2\Big(\frac{y^2-5y-2}{(y-1)^3 y} + \frac{6}{(y-1)^4}\Big)$$

$$\mathcal{K}_7(x) = \frac{3(x^2-1-2x\log(x))}{(x-1)^3}\,,$$

$$\begin{aligned}\mathcal{K}_8(x,y) = -3\Big(&\frac{4}{(x-1)^2(y-1)} + \frac{8x}{(x-1)(y-x)^2} - \frac{4}{(x-1)^2(y-x)}\\ &+ 4x\log(x)\,\mathcal{K}_{10}(x,y) + 4y\log(y)\,\mathcal{K}_{10}(y,x)\Big)\,,\end{aligned}$$

$$\begin{aligned}\mathcal{K}_9(x,y) = 10\Big(&\frac{12x}{(1-x)^2(x-y)^2} - \frac{2x^2-7x-13}{2(x-1)^3(y-1)} - \frac{6(x+1)}{(x-1)^3(y-x)}\\ &- \frac{9(x-3)}{2(x-1)^2(y-1)^2} - \frac{3}{(x-1)(y-1)^3}\\ &+ 3x\log(x)\,\mathcal{K}_{11}(x,y) + 3y\log(y)\,\mathcal{K}_{11}(y,x)\Big)\,,\end{aligned}$$

and

$$\mathcal{K}_{10}(x,y) = \frac{2x}{(x-1)(y-x)^3} + \frac{x-2}{(x-1)^2(y-x)^2}\,,$$

$$\mathcal{K}_{11}(x,y) = \frac{4x}{(x-1)^2(y-x)^3} - \frac{4}{(x-1)^3(y-x)^2} + \frac{x}{(x-1)^4(y-x)}\,.$$

In $h \to Z\gamma$ we used the following loop functions for the amplitude

$$\mathcal{F}_1(x) = 2\left(\frac{x^3-6x^2+3x+6x\log(x)+2}{(x-1)^4}\right)\,,$$

$$\mathcal{F}_2(x) = \frac{2}{3}\left(\frac{x^4-2x^3+9x^2-6x^2\log(x)-10x+2}{x(x-1)^4}\right)\,.$$

A.2 Expanded matrices

Next, we will give the expressions for the coupling matrices, expanded in terms of the vacuum expectation value v. We have the weak isospin matrices T^Q, which read in case of no LQ mixing

$$T^{-1/3} = \begin{pmatrix} 0 & 0 & 0 \\ 0 & -\frac{1}{2} & 0 \\ 0 & 0 & 0 \end{pmatrix}\,,\quad T^{2/3} = \begin{pmatrix} -\frac{1}{2} & 0 & 0 \\ 0 & \frac{1}{2} & 0 \\ 0 & 0 & 1 \end{pmatrix}\,,\quad T^{-4/3} = \begin{pmatrix} 0 & 0 \\ 0 & -1 \end{pmatrix}\,,\quad T^{5/3} = \frac{1}{2}\,, \qquad \text{(A.1)}$$

JHEP11(2020)094

using the basis defined in eq. (2.7). A unitary redefinition of the LQ fields in order to diagonalize the mass matrices in eq. (2.5) also affects the T^Q matrices

$$\tilde{T}^Q = W^Q T^Q W^{Q\dagger}\,. \tag{A.2}$$

Note that the LQ field redefinition has no impact the electromagnetic interaction, since the coupling matrix is proportional to the unit matrix and the W^Q then cancel due to unitarity. If we use the perturbative diagonalization ansatz, we obtain

$$\begin{aligned}
\tilde{T}^{-1/3} &\approx \begin{pmatrix} \frac{-v^2|A_{\tilde{2}1}|^2}{2(m_1^2-\tilde{m}_2^2)^2} & \frac{vA^*_{\tilde{2}1}}{2(\tilde{m}_2^2-m_1^2)} & \frac{v^2A_{3\tilde{2}}A^*_{\tilde{2}1}}{2(m_1^2-\tilde{m}_2^2)(\tilde{m}_2^2-m_3^2)} \\ \frac{vA_{\tilde{2}1}}{2(\tilde{m}_2^2-m_1^2)} & -\frac{1}{2}+\frac{v^2}{2}\left(\frac{|A_{\tilde{2}1}|^2}{(m_1^2-\tilde{m}_2^2)^2}+\frac{|A_{3\tilde{2}}|^2}{(\tilde{m}_2^2-m_3^2)^2}\right) & \frac{vA_{3\tilde{2}}}{2(\tilde{m}_2^2-m_3^2)} \\ \frac{v^2A_{\tilde{2}1}A^*_{3\tilde{2}}}{2(m_1^2-\tilde{m}_2^2)(\tilde{m}_2^2-m_3^2)} & \frac{vA^*_{3\tilde{2}}}{2(\tilde{m}_2^2-m_3^2)} & \frac{-v^2|A_{3\tilde{2}}|^2}{2(\tilde{m}_2^2-m_3^2)^2} \end{pmatrix}, \\
\tilde{T}^{2/3} &\approx \begin{pmatrix} -\frac{1}{2} & \frac{v^2Y_{\tilde{2}2}}{m_2^2-\tilde{m}_2^2} & 0 \\ \frac{v^2Y^*_{\tilde{2}2}}{m_2^2-\tilde{m}_2^2} & \frac{1}{2}+\frac{v^2|A_{3\tilde{2}}|^2}{(\tilde{m}_2^2-m_3^2)^2} & \frac{vA_{3\tilde{2}}}{\sqrt{2}(m_3^2-\tilde{m}_2^2)} \\ 0 & \frac{vA^*_{3\tilde{2}}}{\sqrt{2}(m_3^2-\tilde{m}_2^2)} & 1-\frac{v^2|A_{3\tilde{2}}|^2}{(\tilde{m}_2^2-m_3^2)^2} \end{pmatrix}, \\
\tilde{T}^{-4/3} &\approx \begin{pmatrix} 0 & \frac{\sqrt{2}v^2Y^*_{3\tilde{1}}}{m_3^2-\tilde{m}_1^2} \\ \frac{\sqrt{2}v^2Y_{3\tilde{1}}}{m_3^2-\tilde{m}_1^2} & -1 \end{pmatrix},
\end{aligned} \tag{A.3}$$

valid up to $\mathcal{O}(v^2)$. $T^{5/3}$ is not affected, since the LQ with charge $Q = 5/3$ does not mix. There are also interaction matrices for the $ZZ\Phi^Q\Phi^Q$ vertex, which read in case of no LQ mixing

$$\begin{aligned}
D^{-1/3} &= \begin{pmatrix} \left(\frac{s_w^2}{3}\right)^2 & 0 & 0 \\ 0 & \left(\frac{s_w^2}{3}-\frac{1}{2}\right)^2 & 0 \\ 0 & 0 & \left(\frac{s_w^2}{3}\right)^2 \end{pmatrix} \quad
D^{2/3} = \begin{pmatrix} \left(\frac{2s_w^2}{3}+\frac{1}{2}\right)^2 & 0 & 0 \\ 0 & \left(\frac{2s_w^2}{3}-\frac{1}{2}\right)^2 & 0 \\ 0 & 0 & \left(\frac{2s_w^2}{3}-1\right)^2 \end{pmatrix} \\
D^{-4/3} &= \begin{pmatrix} \left(\frac{4s_w^2}{3}\right)^2 & 0 \\ 0 & \left(\frac{4s_w^2}{3}-1\right)^2 \end{pmatrix} \qquad
D^{5/3} = \left(\frac{5s_w^2}{3}-\frac{1}{2}\right)^2.
\end{aligned} \tag{A.4}$$

JHEP11(2020)094

If we include the LQ mixing, we have

$$
\begin{aligned}
\tilde{D}^{-1/3} &\approx \frac{1}{12}\begin{pmatrix} \frac{4s_w^4}{3}-\frac{(4s_w^2-3)v^2|A_{\tilde{2}1}|^2}{(m_1^2-\tilde{m}_2^2)^2} & \frac{(4s_w^2-3)vA^*_{\tilde{2}1}}{\tilde{m}_2^2-m_1^2} & \frac{(4s_w^2-3)v^2A^*_{\tilde{2}1}A_{3\tilde{2}}}{(m_3^2-\tilde{m}_2^2)(\tilde{m}_2^2-m_1^2)} \\ \frac{(4s_w^2-3)vA_{\tilde{2}1}}{\tilde{m}_2^2-m_1^2} & \tilde{d}_{22} & \frac{(4s_w^2-3)vA_{3\tilde{2}}}{\tilde{m}_2^2-m_3^2} \\ \frac{(4s_w^2-3)v^2A^*_{3\tilde{2}}A_{\tilde{2}1}}{(m_1^2-\tilde{m}_2^2)(\tilde{m}_2^2-m_3^2)} & \frac{(4s_w^2-3)vA^*_{3\tilde{2}}}{\tilde{m}_2^2-m_3^2} & \frac{4s_w^4}{3}-\frac{(4s_w^2-3)v^2|A_{3\tilde{2}}|^2}{(m_3^2-\tilde{m}_2^2)^2} \end{pmatrix}, \\
\text{with}\quad \tilde{d}_{22} &= \frac{(3-2s_w^2)^2}{3}+\frac{(4s_w^2-3)v^2|A_{\tilde{2}1}|^2}{(m_1^2-\tilde{m}_2^2)^2}+\frac{(4s_w^2-3)v^2|A_{3\tilde{2}}|^2}{(m_3^2-\tilde{m}_2^2)^2}, \qquad \text{(A.5)} \\
\tilde{D}^{2/3} &\approx \frac{1}{12}\begin{pmatrix} \frac{(4s_w^2+3)^2}{3} & \frac{16s_w^2v^2Y_{\tilde{2}2}}{\tilde{m}_2^2-m_2^2} & 0 \\ \frac{16s_w^2v^2Y^*_{\tilde{2}2}}{\tilde{m}_2^2-m_2^2} & \frac{(4s_w^2-3)^2}{3}-\frac{2(8s_w^2-9)v^2|A_{3\tilde{2}}|^2}{(m_3^2-\tilde{m}_2^2)^2} & \frac{\sqrt{2}(8s_w^2-9)vA_{3\tilde{2}}}{\tilde{m}_2^2-m_3^2} \\ 0 & \frac{\sqrt{2}(8s_w^2-9)vA^*_{3\tilde{2}}}{\tilde{m}_2^2-m_3^2} & \frac{4(3-2s_w^2)^2}{3}+\frac{2(8s_w^2-9)v^2|A_{3\tilde{2}}|^2}{(m_3^2-\tilde{m}_2^2)^2} \end{pmatrix}, \\
\tilde{D}^{-4/3} &\approx \frac{1}{3}\begin{pmatrix} \frac{16s_w^4}{3} & \frac{\sqrt{2}(8s_w^2-3)v^2Y^*_{31}}{m_3^2-\tilde{m}_1^2} \\ \frac{\sqrt{2}(8s_w^2-3)v^2Y_{31}}{m_3^2-\tilde{m}_1^2} & \frac{(3-4s_w^2)^2}{3} \end{pmatrix}.
\end{aligned}
$$

Analogously to the Z boson, different LQ generations mix under W interactions. Without LQ mixing, the interactions with the W boson can be written in terms of the following matrices

$$
B^1 = \begin{pmatrix} 0 & 0 & 0 \\ 0 & 0 & \sqrt{2} \end{pmatrix}, \qquad B^2 = \begin{pmatrix} 0 & 0 & 0 \\ 0 & 1 & 0 \\ 0 & 0 & -\sqrt{2} \end{pmatrix}, \qquad B^3 = \begin{pmatrix} 1 & 0 & 0 \end{pmatrix}, \qquad \text{(A.6)}
$$

arranging the LQ in their charge eigenstates according to eq. (2.7). B^1 describes the interaction of LQs with electric charges $Q = -4/3$ and $Q = -1/3$, B^2 the ones with $Q = -1/3$ and $Q = 2/3$, B^3 with $Q = 5/3$ and $Q = 2/3$. If we include LQ mixing, the matrices expanded up to $\mathcal{O}(v^2)$, then read

$$
\begin{aligned}
\tilde{B}^1 &\approx \begin{pmatrix} 0 & 0 & \frac{2v^2Y^*_{3\tilde{1}}}{\tilde{m}_1-m_3^2} \\ \frac{\sqrt{2}v^2}{m_1^2-m_3^2}\left(\frac{A_{\tilde{2}1}A^*_{3\tilde{2}}}{m_1^2-\tilde{m}_2^2}+Y^*_{31}\right) & \frac{\sqrt{2}vA^*_{3\tilde{2}}}{\tilde{m}_2^2-m_3^2} & \sqrt{2}-\frac{v^2|A_{3\tilde{2}}|^2}{\sqrt{2}(\tilde{m}_2^2-m_3^2)^2} \end{pmatrix}, \\
\tilde{B}^2 &\approx \begin{pmatrix} 0 & \frac{vA^*_{\tilde{2}1}}{m_1^2-\tilde{m}_2^2} & \frac{\sqrt{2}v^2}{m_1^2-m_3^2}\left(\frac{A_{3\tilde{2}}A^*_{\tilde{2}1}}{m_3^2-\tilde{m}_2^2}-Y_{31}\right) \\ \frac{v^2Y^*_{\tilde{2}2}}{m_2^2-\tilde{m}_2^2} & 1-\frac{v^2}{2}\left(\frac{|A_{\tilde{2}1}|^2}{(m_1^2-\tilde{m}_2^2)^2}-\frac{|A_{3\tilde{2}}|^2}{(\tilde{m}_2^2-m_3^2)^2}\right) & 0 \\ 0 & \frac{vA^*_{3\tilde{2}}}{\tilde{m}_2^2-m_3^2} & -\sqrt{2}-\frac{v^2|A_{3\tilde{2}}|^2}{\sqrt{2}(m_3^2-\tilde{m}_2^2)^2} \end{pmatrix}, \\
\tilde{B}^3 &\approx \begin{pmatrix} 1 & \frac{-v^2Y^*_{\tilde{2}2}}{m_2^2-\tilde{m}_2^2} & 0 \end{pmatrix}. \qquad \text{(A.7)}
\end{aligned}
$$

We also have interaction matrices for the $W^+W^-\Phi^Q\Phi^Q$ vertex. Without mixing, they read

$$
F^{-1/3} = \begin{pmatrix} 0 & 0 & 0 \\ 0 & \frac{1}{2} & 0 \\ 0 & 0 & 2 \end{pmatrix} \qquad F^{2/3} = \begin{pmatrix} \frac{1}{2} & 0 & 0 \\ 0 & \frac{1}{2} & 0 \\ 0 & 0 & 1 \end{pmatrix} \qquad F^{-4/3} = \begin{pmatrix} 0 & 0 \\ 0 & 1 \end{pmatrix}, \qquad F^{5/3} = \frac{1}{2}. \qquad \text{(A.8)}
$$

JHEP11(2020)094

If we include mixing and expand up to order $\mathcal{O}(v^2)$, we obtain

$$\begin{aligned}
\tilde{F}^{-1/3} &\approx \begin{pmatrix} \frac{v^2|A_{\tilde{2}1}|^2}{2(m_1^2-\tilde{m}_2^2)^2} & \frac{vA_{\tilde{2}1}^*}{2(m_1^2-\tilde{m}_2^2)} & \tilde{f}_{13} \\ \frac{vA_{\tilde{2}1}}{2(m_1^2-\tilde{m}_2^2)} & \frac{1}{2}+\frac{v^2}{2}\left(\frac{3|A_{3\tilde{2}}|^2}{(\tilde{m}_2^2-m_3^2)^2}-\frac{|A_{\tilde{2}1}|^2}{(\tilde{m}_2^2-m_1^2)^2}\right) & \frac{3vA_{3\tilde{2}}}{2(\tilde{m}_2^2-m_3^2)}\,, \\ \tilde{f}_{13}^* & \frac{3vA_{3\tilde{2}}^*}{2(\tilde{m}_2^2-m_3^2)} & 2-\frac{3v^2|A_{3\tilde{2}}|^2}{2(\tilde{m}_2^2-m_3^2)^2}\,, \end{pmatrix}, \\
\text{with} \quad \tilde{f}_{13} &= \frac{2v^2 Y_{31}}{m_1^2-m_3^2} - \frac{v^2 A_{3\tilde{2}}A_{\tilde{2}1}^*(m_1^2-4\tilde{m}_2^2+3m_3^2)}{2(m_1^2-m_3^2)(m_1^2-\tilde{m}_2^2)(\tilde{m}_2^2-m_3^2)} \\
\tilde{F}^{2/3} &\approx \begin{pmatrix} \frac{1}{2} & 0 & 0 \\ 0 & \frac{1}{2}+\frac{v^2|A_{3\tilde{2}}|^2}{(\tilde{m}_2^2-m_3^2)^2} & \frac{vA_{3\tilde{2}}}{\sqrt{2}(-m_3^2\tilde{m}_2^2)} \\ 0 & \frac{vA_{3\tilde{2}}^*}{\sqrt{2}(m_3^2-\tilde{m}_2^2)} & 1-\frac{v^2|A_{3\tilde{2}}|^2}{(\tilde{m}_2^2-m_3^2)^2} \end{pmatrix}, \\
\tilde{F}^{-4/3} &\approx \begin{pmatrix} 0 & \frac{\sqrt{2}v^2Y_{3\tilde{1}}^*}{m_1^2-m_3^2} \\ \frac{\sqrt{2}v^2Y_{3\tilde{1}}}{m_1^2-m_3^2} & 1 \end{pmatrix}.
\end{aligned} \tag{A.9}$$

Finally we show the Higgs coupling matrices in (2.13) up to $\mathcal{O}(v)$

$$\begin{aligned}
\tilde{\Gamma}^{-1/3} &\approx \frac{1}{\sqrt{2}} \begin{pmatrix} 2v\left(Y_1+\frac{|A_{\tilde{2}1}|^2}{m_1^2-\tilde{m}_2^2}\right) & A_{\tilde{2}1}^* & v\left(2Y_{31}-\frac{A_{3\tilde{2}}A_{\tilde{2}1}^*(m_1^2+m_3^2-2\tilde{m}_2^2)}{(m_1^2-\tilde{m}_2^2)(\tilde{m}_2^2-m_3^2)}\right) \\ A_{\tilde{2}1} & \tilde{\Gamma}_{22}^{-1/3} & A_{3\tilde{2}} \\ v\left(2Y_{31}^*-\frac{A_{\tilde{2}1}A_{3\tilde{2}}^*(m_1^2+m_3^2-2\tilde{m}_2^2)}{(m_1^2-\tilde{m}_2^2)(\tilde{m}_2^2-m_3^2)}\right) & A_{3\tilde{2}}^* & 2v\left(Y_3+\frac{|A_{3\tilde{2}}|^2}{m_3-\tilde{m}_2^2}\right) \end{pmatrix}, \\
\text{with} \quad \tilde{\Gamma}_{22}^{-1/3} &= 2v\left(Y_{\tilde{2}}-\frac{|A_{\tilde{2}1}|^2}{m_1^2-\tilde{m}_2^2}-\frac{|A_{3\tilde{2}}|^2}{m_3^2-\tilde{m}_2^2}\right), \\
\tilde{\Gamma}^{2/3} &\approx \frac{1}{\sqrt{2}} \begin{pmatrix} 2vY_2 & 2vY_{\tilde{2}2} & 0 \\ 2vY_{\tilde{2}2}^* & 2v\left(Y_{\tilde{2}}+Y_{\tilde{2}\tilde{2}}-\frac{2|A_{3\tilde{2}}|^2}{m_3^2-\tilde{m}_2^2}\right) & -\sqrt{2}A_{3\tilde{2}} \\ 0 & -\sqrt{2}A_{3\tilde{2}}^* & 2v\left(Y_3+\frac{2|A_{3\tilde{2}}|^2}{m_3^2-\tilde{m}_2^2}\right) \end{pmatrix}, \\
\tilde{\Gamma}^{-4/3} &\approx \Gamma^{-4/3}.
\end{aligned} \tag{A.10}$$

and

$$\begin{aligned}
\tilde{\Lambda}^{-1/3} &\approx \frac{1}{2} \begin{pmatrix} Y_1 & v\left(\frac{Y_{31}A_{3\tilde{2}}^*}{\tilde{m}_2^2-m_3^2}+\frac{(Y_{\tilde{2}}-Y_1)A_{\tilde{2}1}^*}{m_1^2-\tilde{m}_2^2}\right) & Y_{31} \\ v\left(\frac{Y_{31}^*A_{3\tilde{2}}}{\tilde{m}_2^2-m_3^2}+\frac{(Y_{\tilde{2}}-Y_1)A_{\tilde{2}1}}{m_1^2-\tilde{m}_2^2}\right) & Y_{\tilde{2}} & v\left(\frac{Y_{31}A_{\tilde{2}1}}{\tilde{m}_2^2-m_1^2}+\frac{(Y_{\tilde{2}}-Y_3)A_{3\tilde{2}}}{m_3^2-\tilde{m}_2^2}\right) \\ Y_{31}^* & v\left(\frac{Y_{31}^*A_{\tilde{2}1}^*}{\tilde{m}_2^2-m_1^2}+\frac{(Y_{\tilde{2}}-Y_3)A_{3\tilde{2}}^*}{m_3^2-\tilde{m}_2^2}\right) & Y_3 \end{pmatrix}, \\
\tilde{\Lambda}^{2/3} &\approx \frac{1}{2} \begin{pmatrix} Y_2 & Y_{\tilde{2}2} & \frac{\sqrt{2}vY_{\tilde{2}2}A_{3\tilde{2}}}{\tilde{m}_2^2-m_3^2} \\ Y_{\tilde{2}2}^* & Y_{\tilde{2}}+Y_{\tilde{2}\tilde{2}} & \frac{\sqrt{2}v(Y_3-Y_{\tilde{2}}-Y_{\tilde{2}\tilde{2}})A_{3\tilde{2}}}{m_3^2-\tilde{m}_2^2} \\ \frac{\sqrt{2}vY_{\tilde{2}2}^*A_{3\tilde{2}}^*}{\tilde{m}_2^2-m_3^2} & \frac{\sqrt{2}v(Y_3-Y_{\tilde{2}}-Y_{\tilde{2}\tilde{2}})A_{3\tilde{2}}^*}{m_3^2-\tilde{m}_2^2} & Y_3 \end{pmatrix}, \\
\tilde{\Lambda}^{-4/3} &\approx \Lambda^{-4/3}.
\end{aligned} \tag{A.11}$$

JHEP11(2020)094

A.3 Exact results for the vacuum polarization functions

In this section we give the q^2-expanded results for the vacuum polarization functions, with the LQ masses and couplings kept unexpanded

$$
\begin{aligned}
\Pi_{\gamma\gamma}(q^2) &= -\sum_Q \frac{N_c\, e^2 Q^2}{48\pi^2} q^2 \left(\frac{1}{\varepsilon} + \log\left(\frac{\mu^2}{\left(M_a^Q\right)^2}\right) + \frac{q^2}{10\left(M_a^Q\right)^2}\right) , \\
\Pi_{Z\gamma}(q^2) &= -\sum_Q \frac{N_c\, g_2 e \left(\tilde{T}^Q_{aa} - s_w^2 Q\right) Q}{48\pi^2 c_w} q^2 \left(\frac{1}{\varepsilon} + \log\left(\frac{\mu^2}{\left(M_a^Q\right)^2}\right) + \frac{q^2}{10\left(M_a^Q\right)^2}\right) , \\
\Pi_{ZZ}(q^2) &= \sum_Q \frac{N_c}{16\pi^2}\left(\frac{g_2 \Gamma^Q_{aa}}{c_w}\frac{m_Z}{m_h^2} - \frac{2 g_2^2 \tilde{D}^Q_{aa}}{c_w^2}\right)\left(M_a^Q\right)^2 \left(\frac{1}{\varepsilon} + \log\left(\frac{\mu^2}{\left(M_a^Q\right)^2}\right) + 1\right) \\
&\quad - \sum_Q \frac{N_c\, g_2^2 \left(\tilde{T}^Q_{ab} - s_w^2 Q \delta_{ab}\right)\left(\tilde{T}^Q_{ba} - s_w^2 Q \delta_{ba}\right)}{32\pi^2 c_w^2} \times F\left(\left(M_a^Q\right)^2, \left(M_b^Q\right)^2\right) , \\
\Pi_{WW}(q^2) &= \sum_Q \frac{N_c}{16\pi^2}\left(g_2 \Gamma^Q_{aa}\frac{m_W}{m_h^2} - g_2^2 \tilde{F}^Q_{aa}\right)\left(M_a^Q\right)^2 \left(\frac{1}{\varepsilon} + \log\left(\frac{\mu^2}{\left(M_a^Q\right)^2}\right) + 1\right) \\
&\quad - \sum_{a(b)=1}^{2(3)} \frac{N_c\, g_2^2 \left|\tilde{B}^1_{ab}\right|^2}{64\pi^2}\left(M_a^{-4/3}\right)^2 F\left(\left(M_a^{-4/3}\right)^2, \left(M_b^{-1/3}\right)^2\right) \\
&\quad - \sum_{a,b=1}^{3} \frac{N_c\, g_2^2 \left|\tilde{B}^2_{ab}\right|^2}{64\pi^2}\left(M_a^{-1/3}\right)^2 F\left(\left(M_a^{-1/3}\right)^2, \left(M_b^{2/3}\right)^2\right) \\
&\quad - \sum_{b=1}^{3} \frac{N_c\, g_2^2 \left|\tilde{B}^3_{b}\right|^2}{64\pi^2}\left(M^{5/3}\right)^2 F\left(\left(M^{5/3}\right)^2, \left(M_b^{2/3}\right)^2\right) ,
\end{aligned}
\tag{A.12}
$$

where $Q = \{-1/3, 2/3, -4/3, 5/3\}$ with a and b running from 1 to 3, 3, 2, and 1, respectively. Here we defined

$$
F\left(\left(M_a^Q\right)^2, \left(M_b^Q\right)^2\right) = \left(M_a^Q\right)^2 \left(f_0 + \frac{q^2}{\left(M_a^Q\right)^2} f_1 + \left(\frac{q^2}{\left(M_a^Q\right)^2}\right)^2 f_2\right) , \tag{A.13}
$$

with

$$
\begin{aligned}
f_0 &= -2(x^Q_{ba}+1)\left(\frac{1}{\varepsilon} + \log\left(\frac{\mu^2}{M_a^2}\right) + \frac{3}{2}\right) + \frac{2(x^Q_{ba})^2 \log(x^Q_{ba})}{x^Q_{ba}-1} , \\
f_1 &= \frac{2}{3}\left(\frac{1}{\varepsilon} + \log\left(\frac{\mu^2}{M_a^2}\right)\right) - \frac{5 - 27x^Q_{ba} + 27(x^Q_{ba})^2 - 5(x^Q_{ba})^3 - 6(3 - x^Q_{ba})(x^Q_{ba})^2 \log(x^Q_{ba})}{9(x^Q_{ba}-1)^3} , \\
f_2 &= \frac{-1 + 8x^Q_{ba} - 8(x^Q_{ba})^3 + (x^Q_{ba})^4 + 12(x^Q_{ba})^2 \log(x^Q_{ba})}{6(x^Q_{ba}-1)^5} ,
\end{aligned}
\tag{A.14}
$$

where again

$$
x^Q_{ba} = \frac{\left(M_b^Q\right)^2}{\left(M_a^Q\right)^2} .
$$

JHEP11(2020)094

A.4 Leading order SM amplitudes in Higgs decays

The SM amplitudes for the $h\gamma\gamma$, hgg and $hZ\gamma$ couplings in eq. (4.6) read

$$\begin{aligned}
A_1(x) &= \frac{-(2x^2+3x+3(2x-1)f(x))}{x^2}\,,\\
A_{1/2}(x) &= \frac{2(x+(x-1)f(x))}{x^2}\\
C_1(x,y) &= 4(3-\frac{s_w^2}{c_w^2})I_2(x,y) + \Big((1+\frac{2}{x})\frac{s_w^2}{c_w^2} - (5+\frac{2}{x})\Big)I_1(x,y)\,,\\
C_{1/2}(x,y) &= I_1(x,y) - I_2(x,y)\,,
\end{aligned} \tag{A.15}$$

with

$$\begin{aligned}
f(x) &= \arcsin^2(\sqrt{x})\,,\\
g(x) &= \sqrt{\frac{1}{x}-1}\,\arcsin(\sqrt{x})\,,\\
I_1(x,y) &= \frac{xy}{2(x-y)} + \frac{x^2y^2(f(x^{-1})-f(y^{-1}))}{2(x-y)^2} + \frac{x^2y(g(x^{-1})-g(y^{-1}))}{(x-y)^2}\,,\\
I_2(x,y) &= \frac{-xy(f(x^{-1})-f(y^{-1}))}{2(x-y)}\,.
\end{aligned} \tag{A.16}$$

Open Access. This article is distributed under the terms of the Creative Commons Attribution License (CC-BY 4.0), which permits any use, distribution and reproduction in any medium, provided the original author(s) and source are credited.

References

[1] J.C. Pati and A. Salam, *Lepton number as the fourth color*, Phys. Rev. D **10** (1974) 275 [*Erratum ibid.* **11** (1975) 703] [INSPIRE].

[2] H. Georgi and S.L. Glashow, *Unity of all elementary particle forces*, Phys. Rev. Lett. **32** (1974) 438 [INSPIRE].

[3] H. Georgi, H.R. Quinn and S. Weinberg, *Hierarchy of interactions in unified gauge theories*, Phys. Rev. Lett. **33** (1974) 451 [INSPIRE].

[4] H. Fritzsch and P. Minkowski, *Unified interactions of leptons and hadrons*, Annals Phys. **93** (1975) 193 [INSPIRE].

[5] W. Buchmüller, R. Ruckl and D. Wyler, *Leptoquarks in lepton-quark collisions*, Phys. Lett. B **191** (1987) 442 [*Erratum ibid.* **448** (1999) 320] [INSPIRE].

[6] BaBar collaboration, *Evidence for an excess of $\bar{B} \to D^{(*)}\tau^-\bar{\nu}_\tau$ decays*, Phys. Rev. Lett. **109** (2012) 101802 [arXiv:1205.5442] [INSPIRE].

[7] BaBar collaboration, *Measurement of an excess of $\bar{B} \to D^{(*)}\tau^-\bar{\nu}_\tau$ decays and implications for charged Higgs bosons*, Phys. Rev. D **88** (2013) 072012 [arXiv:1303.0571] [INSPIRE].

[8] LHCb collaboration, *Measurement of the ratio of branching fractions $\mathcal{B}(\bar{B}^0 \to D^{*+}\tau^-\bar{\nu}_\tau)/\mathcal{B}(\bar{B}^0 \to D^{*+}\mu^-\bar{\nu}_\mu)$*, Phys. Rev. Lett. **115** (2015) 111803 [*Erratum ibid.* **115** (2015) 159901] [arXiv:1506.08614] [INSPIRE].

[9] LHCb collaboration, *Test of lepton flavor universality by the measurement of the $B^0 \to D^{*-}\tau^+\nu_\tau$ branching fraction using three-prong τ decays*, Phys. Rev. D **97** (2018) 072013 [arXiv:1711.02505] [INSPIRE].

[10] LHCb collaboration, *Measurement of the ratio of the $B^0 \to D^{*-}\tau^+\nu_\tau$ and $B^0 \to D^{*-}\mu^+\nu_\mu$ branching fractions using three-prong τ-lepton decays*, Phys. Rev. Lett. **120** (2018) 171802 [arXiv:1708.08856] [INSPIRE].

[11] Belle collaboration, *Measurement of $\mathcal{R}(D)$ and $\mathcal{R}(D^*)$ with a semileptonic tagging method*, arXiv:1904.08794 [INSPIRE].

[12] CMS and LHCb collaborations, *Observation of the rare $B_s^0 \to \mu^+\mu^-$ decay from the combined analysis of CMS and LHCb data*, Nature **522** (2015) 68 [arXiv:1411.4413] [INSPIRE].

[13] LHCb collaboration, *Angular analysis of the $B^0 \to K^{*0}\mu^+\mu^-$ decay using 3 fb^{-1} of integrated luminosity*, JHEP **02** (2016) 104 [arXiv:1512.04442] [INSPIRE].

[14] Belle collaboration, *Angular analysis of $B^0 \to K^*(892)^0\ell^+\ell^-$*, in *LHC ski* 2016*: a first discussion of* 13 *TeV results*, (2016) [arXiv:1604.04042] [INSPIRE].

[15] LHCb collaboration, *Test of lepton universality with $B^0 \to K^{*0}\ell^+\ell^-$ decays*, JHEP **08** (2017) 055 [arXiv:1705.05802] [INSPIRE].

[16] LHCb collaboration, *Search for lepton-universality violation in $B^+ \to K^+\ell^+\ell^-$ decays*, Phys. Rev. Lett. **122** (2019) 191801 [arXiv:1903.09252] [INSPIRE].

[17] LHCb collaboration, *Measurement of CP-averaged observables in the $B^0 \to K^{*0}\mu^+\mu^-$ decay*, Phys. Rev. Lett. **125** (2020) 011802 [arXiv:2003.04831] [INSPIRE].

[18] Muon g-2 collaboration, *Final report of the muon E*821 *anomalous magnetic moment measurement at BNL*, Phys. Rev. D **73** (2006) 072003 [hep-ex/0602035] [INSPIRE].

[19] HFLAV collaboration, *Averages of b-hadron, c-hadron, and τ-lepton properties as of summer* 2016, Eur. Phys. J. C **77** (2017) 895 [arXiv:1612.07233] [INSPIRE].

[20] C. Murgui, A. Peñuelas, M. Jung and A. Pich, *Global fit to $b \to c\tau\nu$ transitions*, JHEP **09** (2019) 103 [arXiv:1904.09311] [INSPIRE].

[21] R.-X. Shi, L.-S. Geng, B. Grinstein, S. Jäger and J. Martin Camalich, *Revisiting the new-physics interpretation of the $b \to c\tau\nu$ data*, JHEP **12** (2019) 065 [arXiv:1905.08498] [INSPIRE].

[22] M. Blanke, A. Crivellin, T. Kitahara, M. Moscati, U. Nierste and I. Nišandžić, *Addendum to "Impact of polarization observables and $B_c \to \tau\nu$ on new physics explanations of the $b \to c\tau\nu$ anomaly"*, Phys. Rev. D **100** (2019) 035035 [arXiv:1905.08253] [INSPIRE].

[23] S. Kumbhakar, A.K. Alok, D. Kumar and S.U. Sankar, *A global fit to $b \to c\tau\bar{\nu}$ anomalies after Moriond* 2019, in 2019 *European Physical Society Conference on High Energy Physics*, (2019) [arXiv:1909.02840] [INSPIRE].

[24] B. Capdevila, A. Crivellin, S. Descotes-Genon, J. Matias and J. Virto, *Patterns of new physics in $b \to s\ell^+\ell^-$ transitions in the light of recent data*, JHEP **01** (2018) 093 [arXiv:1704.05340] [INSPIRE].

[25] W. Altmannshofer, P. Stangl and D.M. Straub, *Interpreting hints for lepton flavor universality violation*, Phys. Rev. D **96** (2017) 055008 [arXiv:1704.05435] [INSPIRE].

[26] M. Algueró et al., *Emerging patterns of new physics with and without lepton flavour universal contributions*, *Eur. Phys. J. C* **79** (2019) 714 [*Addendum ibid.* **80** (2020) 511] [arXiv:1903.09578] [INSPIRE].

[27] A.K. Alok, A. Dighe, S. Gangal and D. Kumar, *Continuing search for new physics in $b \to s\mu\mu$ decays: two operators at a time*, *JHEP* **06** (2019) 089 [arXiv:1903.09617] [INSPIRE].

[28] M. Ciuchini et al., *New physics in $b \to s\ell^+\ell^-$ confronts new data on lepton universality*, *Eur. Phys. J. C* **79** (2019) 719 [arXiv:1903.09632] [INSPIRE].

[29] J. Aebischer, W. Altmannshofer, D. Guadagnoli, M. Reboud, P. Stangl and D.M. Straub, *B-decay discrepancies after Moriond* 2019, *Eur. Phys. J. C* **80** (2020) 252 [arXiv:1903.10434] [INSPIRE].

[30] A. Arbey, T. Hurth, F. Mahmoudi, D.M. Santos and S. Neshatpour, *Update on the $b \to s$ anomalies*, *Phys. Rev. D* **100** (2019) 015045 [arXiv:1904.08399] [INSPIRE].

[31] D. Kumar, K. Kowalska and E.M. Sessolo, *Global Bayesian analysis of new physics in $b \to s\mu\mu$ transitions after Moriond*-2019, in 17$^{\rm th}$ *conference on flavor physics and CP-violation*, (2019) [arXiv:1906.08596] [INSPIRE].

[32] T. Aoyama et al., *The anomalous magnetic moment of the muon in the Standard Model*, arXiv:2006.04822 [INSPIRE].

[33] R. Alonso, B. Grinstein and J. Martin Camalich, *Lepton universality violation and lepton flavor conservation in B-meson decays*, *JHEP* **10** (2015) 184 [arXiv:1505.05164] [INSPIRE].

[34] L. Calibbi, A. Crivellin and T. Ota, *Effective field theory approach to $b \to s\ell\ell^{(\prime)}$, $B \to K^{(*)}\nu\bar{\nu}$ and $B \to D^{(*)}\tau\nu$ with third generation couplings*, *Phys. Rev. Lett.* **115** (2015) 181801 [arXiv:1506.02661] [INSPIRE].

[35] G. Hiller, D. Loose and K. Schönwald, *Leptoquark flavor patterns & B decay anomalies*, *JHEP* **12** (2016) 027 [arXiv:1609.08895] [INSPIRE].

[36] B. Bhattacharya, A. Datta, J.-P. Guévin, D. London and R. Watanabe, *Simultaneous explanation of the R_K and $R_{D^{(*)}}$ puzzles: a model analysis*, *JHEP* **01** (2017) 015 [arXiv:1609.09078] [INSPIRE].

[37] D. Buttazzo, A. Greljo, G. Isidori and D. Marzocca, *B-physics anomalies: a guide to combined explanations*, *JHEP* **11** (2017) 044 [arXiv:1706.07808] [INSPIRE].

[38] R. Barbieri, G. Isidori, A. Pattori and F. Senia, *Anomalies in B-decays and* U(2) *flavour symmetry*, *Eur. Phys. J. C* **76** (2016) 67 [arXiv:1512.01560] [INSPIRE].

[39] R. Barbieri, C.W. Murphy and F. Senia, *B-decay anomalies in a composite leptoquark model*, *Eur. Phys. J. C* **77** (2017) 8 [arXiv:1611.04930] [INSPIRE].

[40] L. Calibbi, A. Crivellin and T. Li, *Model of vector leptoquarks in view of the B-physics anomalies*, *Phys. Rev. D* **98** (2018) 115002 [arXiv:1709.00692] [INSPIRE].

[41] A. Crivellin, D. Müller, A. Signer and Y. Ulrich, *Correlating lepton flavor universality violation in B decays with $\mu \to e\gamma$ using leptoquarks*, *Phys. Rev. D* **97** (2018) 015019 [arXiv:1706.08511] [INSPIRE].

[42] M. Bordone, C. Cornella, J. Fuentes-Martín and G. Isidori, *Low-energy signatures of the* PS^3 *model: from B-physics anomalies to LFV*, *JHEP* **10** (2018) 148 [arXiv:1805.09328] [INSPIRE].

[43] J. Kumar, D. London and R. Watanabe, *Combined explanations of the* $b \to s\mu^+\mu^-$ *and* $b \to c\tau^-\bar{\nu}$ *anomalies: a general model analysis*, *Phys. Rev. D* **99** (2019) 015007 [arXiv:1806.07403] [INSPIRE].

[44] A. Crivellin, C. Greub, D. Müller and F. Saturnino, *Importance of loop effects in explaining the accumulated evidence for new physics in B decays with a vector leptoquark*, *Phys. Rev. Lett.* **122** (2019) 011805 [arXiv:1807.02068] [INSPIRE].

[45] A. Crivellin and F. Saturnino, *Explaining the flavor anomalies with a vector leptoquark (Moriond* 2019 *update)*, PoS(DIS2019)163 (2019) [arXiv:1906.01222] [INSPIRE].

[46] C. Cornella, J. Fuentes-Martin and G. Isidori, *Revisiting the vector leptoquark explanation of the B-physics anomalies*, *JHEP* **07** (2019) 168 [arXiv:1903.11517] [INSPIRE].

[47] M. Bordone, O. Catà and T. Feldmann, *Effective theory approach to new physics with flavour: general framework and a leptoquark example*, *JHEP* **01** (2020) 067 [arXiv:1910.02641] [INSPIRE].

[48] J. Bernigaud, I. de Medeiros Varzielas and J. Talbert, *Finite family groups for fermionic and leptoquark mixing patterns*, *JHEP* **01** (2020) 194 [arXiv:1906.11270] [INSPIRE].

[49] J. Aebischer, A. Crivellin and C. Greub, *QCD improved matching for semileptonic B decays with leptoquarks*, *Phys. Rev. D* **99** (2019) 055002 [arXiv:1811.08907] [INSPIRE].

[50] J. Fuentes-Martín, G. Isidori, M. König and N. Selimović, *Vector leptoquarks beyond tree level*, *Phys. Rev. D* **101** (2020) 035024 [arXiv:1910.13474] [INSPIRE].

[51] S. Fajfer and N. Košnik, *Vector leptoquark resolution of* R_K *and* $R_{D^{(*)}}$ *puzzles*, *Phys. Lett. B* **755** (2016) 270 [arXiv:1511.06024] [INSPIRE].

[52] M. Blanke and A. Crivellin, *B meson anomalies in a Pati-Salam model within the Randall-Sundrum background*, *Phys. Rev. Lett.* **121** (2018) 011801 [arXiv:1801.07256] [INSPIRE].

[53] I. de Medeiros Varzielas and J. Talbert, *Simplified models of flavourful leptoquarks*, *Eur. Phys. J. C* **79** (2019) 536 [arXiv:1901.10484] [INSPIRE].

[54] I. de Medeiros Varzielas and G. Hiller, *Clues for flavor from rare lepton and quark decays*, *JHEP* **06** (2015) 072 [arXiv:1503.01084] [INSPIRE].

[55] A. Crivellin, D. Müller and F. Saturnino, *Flavor phenomenology of the leptoquark singlet-triplet model*, *JHEP* **06** (2020) 020 [arXiv:1912.04224] [INSPIRE].

[56] S. Saad, *Combined explanations of* $(g-2)_\mu$, $R_{D^{(*)}}$, $R_{K^{(*)}}$ *anomalies in a two-loop radiative neutrino mass model*, *Phys. Rev. D* **102** (2020) 015019 [arXiv:2005.04352] [INSPIRE].

[57] S. Saad and A. Thapa, *Common origin of neutrino masses and* $R_{D^{(*)}}$, $R_{K^{(*)}}$ *anomalies*, *Phys. Rev. D* **102** (2020) 015014 [arXiv:2004.07880] [INSPIRE].

[58] M. Bordone, C. Cornella, J. Fuentes-Martin and G. Isidori, *A three-site gauge model for flavor hierarchies and flavor anomalies*, *Phys. Lett. B* **779** (2018) 317 [arXiv:1712.01368] [INSPIRE].

[59] A. Biswas, D. Kumar Ghosh, N. Ghosh, A. Shaw and A.K. Swain, *Collider signature of U_1 leptoquark and constraints from $b \to c$ observables*, *J. Phys. G* **47** (2020) 045005 [arXiv:1808.04169] [INSPIRE].

[60] J. Heeck and D. Teresi, *Pati-Salam explanations of the B-meson anomalies*, *JHEP* **12** (2018) 103 [arXiv:1808.07492] [INSPIRE].

[61] S. Sahoo and R. Mohanta, *Scalar leptoquarks and the rare B meson decays*, *Phys. Rev. D* **91** (2015) 094019 [arXiv:1501.05193] [INSPIRE].

[62] C.-H. Chen, T. Nomura and H. Okada, *Explanation of $B \to K^{(*)}\ell^+\ell^-$ and muon $g-2$, and implications at the LHC*, *Phys. Rev. D* **94** (2016) 115005 [arXiv:1607.04857] [INSPIRE].

[63] U.K. Dey, D. Kar, M. Mitra, M. Spannowsky and A.C. Vincent, *Searching for leptoquarks at IceCube and the LHC*, *Phys. Rev. D* **98** (2018) 035014 [arXiv:1709.02009] [INSPIRE].

[64] D. Bečirević and O. Sumensari, *A leptoquark model to accommodate $R_K^{\rm exp} < R_K^{\rm SM}$ and $R_{K^*}^{\rm exp} < R_{K^*}^{\rm SM}$*, *JHEP* **08** (2017) 104 [arXiv:1704.05835] [INSPIRE].

[65] B. Chauhan, B. Kindra and A. Narang, *Discrepancies in simultaneous explanation of flavor anomalies and IceCube PeV events using leptoquarks*, *Phys. Rev. D* **97** (2018) 095007 [arXiv:1706.04598] [INSPIRE].

[66] D. Bečirević, I. Doršner, S. Fajfer, N. Košnik, D.A. Faroughy and O. Sumensari, *Scalar leptoquarks from grand unified theories to accommodate the B-physics anomalies*, *Phys. Rev. D* **98** (2018) 055003 [arXiv:1806.05689] [INSPIRE].

[67] O. Popov, M.A. Schmidt and G. White, *R_2 as a single leptoquark solution to $R_{D^{(*)}}$ and $R_{K^{(*)}}$*, *Phys. Rev. D* **100** (2019) 035028 [arXiv:1905.06339] [INSPIRE].

[68] S. Fajfer, J.F. Kamenik, I. Nisandzic and J. Zupan, *Implications of lepton flavor universality violations in B decays*, *Phys. Rev. Lett.* **109** (2012) 161801 [arXiv:1206.1872] [INSPIRE].

[69] N.G. Deshpande and A. Menon, *Hints of R-parity violation in B decays into $\tau\nu$*, *JHEP* **01** (2013) 025 [arXiv:1208.4134] [INSPIRE].

[70] M. Freytsis, Z. Ligeti and J.T. Ruderman, *Flavor models for $\bar{B} \to D^{(*)}\tau\bar{\nu}$*, *Phys. Rev. D* **92** (2015) 054018 [arXiv:1506.08896] [INSPIRE].

[71] M. Bauer and M. Neubert, *Minimal leptoquark explanation for the $R_{D^{(*)}}$, R_K, and $(g-2)_g$ anomalies*, *Phys. Rev. Lett.* **116** (2016) 141802 [arXiv:1511.01900] [INSPIRE].

[72] X.-Q. Li, Y.-D. Yang and X. Zhang, *Revisiting the one leptoquark solution to the $R(D^{(*)})$ anomalies and its phenomenological implications*, *JHEP* **08** (2016) 054 [arXiv:1605.09308] [INSPIRE].

[73] J. Zhu, H.-M. Gan, R.-M. Wang, Y.-Y. Fan, Q. Chang and Y.-G. Xu, *Probing the R-parity violating supersymmetric effects in the exclusive $b \to c\ell^-\bar{\nu}_\ell$ decays*, *Phys. Rev. D* **93** (2016) 094023 [arXiv:1602.06491] [INSPIRE].

[74] O. Popov and G.A. White, *One leptoquark to unify them? Neutrino masses and unification in the light of $(g-2)_\mu$, $R_{D^{(*)}}$ and R_K anomalies*, *Nucl. Phys. B* **923** (2017) 324 [arXiv:1611.04566] [INSPIRE].

[75] N.G. Deshpande and X.-G. He, *Consequences of R-parity violating interactions for anomalies in $\bar{B} \to D^{(*)}\tau\bar{\nu}$ and $b \to s\mu^+\mu^-$*, *Eur. Phys. J. C* **77** (2017) 134 [arXiv:1608.04817] [INSPIRE].

JHEP11(2020)094

[76] D. Bečirević, N. Košnik, O. Sumensari and R. Zukanovich Funchal, *Palatable leptoquark scenarios for lepton flavor violation in exclusive $b \to s\ell_1\ell_2$ modes*, JHEP **11** (2016) 035 [arXiv:1608.07583] [INSPIRE].

[77] Y. Cai, J. Gargalionis, M.A. Schmidt and R.R. Volkas, *Reconsidering the one leptoquark solution: flavor anomalies and neutrino mass*, JHEP **10** (2017) 047 [arXiv:1704.05849] [INSPIRE].

[78] W. Altmannshofer, P.S. Bhupal Dev and A. Soni, *$R_{D^{(*)}}$ anomaly: a possible hint for natural supersymmetry with R-parity violation*, Phys. Rev. D **96** (2017) 095010 [arXiv:1704.06659] [INSPIRE].

[79] S. Kamali, A. Rashed and A. Datta, *New physics in inclusive $B \to X_c\ell\bar{\nu}$ decay in light of $R(D^{(*)})$ measurements*, Phys. Rev. D **97** (2018) 095034 [arXiv:1801.08259] [INSPIRE].

[80] A. Azatov, D. Bardhan, D. Ghosh, F. Sgarlata and E. Venturini, *Anatomy of $b \to c\tau\nu$ anomalies*, JHEP **11** (2018) 187 [arXiv:1805.03209] [INSPIRE].

[81] J. Zhu, B. Wei, J.-H. Sheng, R.-M. Wang, Y. Gao and G.-R. Lu, *Probing the R-parity violating supersymmetric effects in $B_c \to J/\psi\ell^-\bar{\nu}_\ell, \eta_c\ell^-\bar{\nu}_\ell$ and $\Lambda_b \to \Lambda_c\ell^-\bar{\nu}_\ell$ decays*, Nucl. Phys. B **934** (2018) 380 [arXiv:1801.00917] [INSPIRE].

[82] A. Angelescu, D. Bečirević, D.A. Faroughy and O. Sumensari, *Closing the window on single leptoquark solutions to the B-physics anomalies*, JHEP **10** (2018) 183 [arXiv:1808.08179] [INSPIRE].

[83] T.J. Kim, P. Ko, J. Li, J. Park and P. Wu, *Correlation between $R_{D^{(*)}}$ and top quark FCNC decays in leptoquark models*, JHEP **07** (2019) 025 [arXiv:1812.08484] [INSPIRE].

[84] A. Crivellin and F. Saturnino, *Correlating tauonic B decays with the neutron electric dipole moment via a scalar leptoquark*, Phys. Rev. D **100** (2019) 115014 [arXiv:1905.08257] [INSPIRE].

[85] H. Yan, Y.-D. Yang and X.-B. Yuan, *Phenomenology of $b \to c\tau\bar{\nu}$ decays in a scalar leptoquark model*, Chin. Phys. C **43** (2019) 083105 [arXiv:1905.01795] [INSPIRE].

[86] A. Crivellin, D. Müller and T. Ota, *Simultaneous explanation of $R(D^{(*)})$ and $b \to s\mu^+\mu^-$: the last scalar leptoquarks standing*, JHEP **09** (2017) 040 [arXiv:1703.09226] [INSPIRE].

[87] D. Marzocca, *Addressing the B-physics anomalies in a fundamental composite Higgs model*, JHEP **07** (2018) 121 [arXiv:1803.10972] [INSPIRE].

[88] I. Bigaran, J. Gargalionis and R.R. Volkas, *A near-minimal leptoquark model for reconciling flavour anomalies and generating radiative neutrino masses*, JHEP **10** (2019) 106 [arXiv:1906.01870] [INSPIRE].

[89] P.S.B. Dev, R. Mohanta, S. Patra and S. Sahoo, *Unified explanation of flavor anomalies, radiative neutrino mass and ANITA anomalous events in a vector leptoquark model*, arXiv:2004.09464 [INSPIRE].

[90] W. Altmannshofer, P.S.B. Dev, A. Soni and Y. Sui, *Addressing $R_{D^{(*)}}$, $R_{K^{(*)}}$, muon $g-2$ and ANITA anomalies in a minimal R-parity violating supersymmetric framework*, Phys. Rev. D **102** (2020) 015031 [arXiv:2002.12910] [INSPIRE].

[91] A. Djouadi, T. Kohler, M. Spira and J. Tutas, *(eb), (et) type leptoquarks at ep colliders*, Z. Phys. C **46** (1990) 679 [INSPIRE].

JHEP11(2020)094

[92] D. Chakraverty, D. Choudhury and A. Datta, *A nonsupersymmetric resolution of the anomalous muon magnetic moment*, *Phys. Lett. B* **506** (2001) 103 [hep-ph/0102180] [INSPIRE].

[93] K.-M. Cheung, *Muon anomalous magnetic moment and leptoquark solutions*, *Phys. Rev. D* **64** (2001) 033001 [hep-ph/0102238] [INSPIRE].

[94] C. Biggio, M. Bordone, L. Di Luzio and G. Ridolfi, *Massive vectors and loop observables: the $g-2$ case*, *JHEP* **10** (2016) 002 [arXiv:1607.07621] [INSPIRE].

[95] S. Davidson, D.C. Bailey and B.A. Campbell, *Model independent constraints on leptoquarks from rare processes*, *Z. Phys. C* **61** (1994) 613 [hep-ph/9309310] [INSPIRE].

[96] G. Couture and H. Konig, *Bounds on second generation scalar leptoquarks from the anomalous magnetic moment of the muon*, *Phys. Rev. D* **53** (1996) 555 [hep-ph/9507263] [INSPIRE].

[97] U. Mahanta, *Implications of BNL measurement of δa_μ on a class of scalar leptoquark interactions*, *Eur. Phys. J. C* **21** (2001) 171 [hep-ph/0102176] [INSPIRE].

[98] F.S. Queiroz, K. Sinha and A. Strumia, *Leptoquarks, dark matter, and anomalous LHC events*, *Phys. Rev. D* **91** (2015) 035006 [arXiv:1409.6301] [INSPIRE].

[99] E. Coluccio Leskow, G. D'Ambrosio, A. Crivellin and D. Müller, *$(g-2)_\mu$, lepton flavor violation, and Z decays with leptoquarks: correlations and future prospects*, *Phys. Rev. D* **95** (2017) 055018 [arXiv:1612.06858] [INSPIRE].

[100] C.-H. Chen, T. Nomura and H. Okada, *Excesses of muon $g-2$, $R_{D^{(*)}}$, and R_K in a leptoquark model*, *Phys. Lett. B* **774** (2017) 456 [arXiv:1703.03251] [INSPIRE].

[101] D. Das, C. Hati, G. Kumar and N. Mahajan, *Towards a unified explanation of $R_{D^{(*)}}$, R_K and $(g-2)_\mu$ anomalies in a left-right model with leptoquarks*, *Phys. Rev. D* **94** (2016) 055034 [arXiv:1605.06313] [INSPIRE].

[102] A. Crivellin, M. Hoferichter and P. Schmidt-Wellenburg, *Combined explanations of $(g-2)_{\mu,e}$ and implications for a large muon EDM*, *Phys. Rev. D* **98** (2018) 113002 [arXiv:1807.11484] [INSPIRE].

[103] K. Kowalska, E.M. Sessolo and Y. Yamamoto, *Constraints on charmphilic solutions to the muon $g-2$ with leptoquarks*, *Phys. Rev. D* **99** (2019) 055007 [arXiv:1812.06851] [INSPIRE].

[104] R. Mandal and A. Pich, *Constraints on scalar leptoquarks from lepton and kaon physics*, *JHEP* **12** (2019) 089 [arXiv:1908.11155] [INSPIRE].

[105] I. Doršner, S. Fajfer and O. Sumensari, *Muon $g-2$ and scalar leptoquark mixing*, *JHEP* **06** (2020) 089 [arXiv:1910.03877] [INSPIRE].

[106] L. Delle Rose, C. Marzo and L. Marzola, *Simplified leptoquark models for precision $l_i \to l_f \gamma$ experiments: two-loop structure of $O(\alpha_S Y^2)$ corrections*, arXiv:2005.12389 [INSPIRE].

[107] I. Bigaran and R.R. Volkas, *Getting chirality right: single scalar leptoquark solution/s to the $(g-2)_{e,\mu}$ puzzle*, *Phys. Rev. D* **102** (2020) 075037 [arXiv:2002.12544] [INSPIRE].

[108] M. Krämer, T. Plehn, M. Spira and P.M. Zerwas, *Pair production of scalar leptoquarks at the Tevatron*, *Phys. Rev. Lett.* **79** (1997) 341 [hep-ph/9704322] [INSPIRE].

[109] M. Krämer, T. Plehn, M. Spira and P.M. Zerwas, *Pair production of scalar leptoquarks at the CERN LHC*, *Phys. Rev. D* **71** (2005) 057503 [hep-ph/0411038] [INSPIRE].

[110] D.A. Faroughy, A. Greljo and J.F. Kamenik, *Confronting lepton flavor universality violation in B decays with high-p_T tau lepton searches at LHC*, Phys. Lett. B **764** (2017) 126 [arXiv:1609.07138] [INSPIRE].

[111] A. Greljo and D. Marzocca, *High-p_T dilepton tails and flavor physics*, Eur. Phys. J. C **77** (2017) 548 [arXiv:1704.09015] [INSPIRE].

[112] I. Doršner, S. Fajfer, D.A. Faroughy and N. Košnik, *The role of the S_3 GUT leptoquark in flavor universality and collider searches*, JHEP **10** (2017) 188 [arXiv:1706.07779] [INSPIRE].

[113] A. Cerri et al., *Report from working group 4: opportunities in flavour physics at the HL-LHC and HE-LHC*, CERN Yellow Rep. Monogr. **7** (2019) 867 [arXiv:1812.07638] [INSPIRE].

[114] P. Bandyopadhyay and R. Mandal, *Revisiting scalar leptoquark at the LHC*, Eur. Phys. J. C **78** (2018) 491 [arXiv:1801.04253] [INSPIRE].

[115] G. Hiller, D. Loose and I. Nišandžić, *Flavorful leptoquarks at hadron colliders*, Phys. Rev. D **97** (2018) 075004 [arXiv:1801.09399] [INSPIRE].

[116] T. Faber et al., *Collider phenomenology of a unified leptoquark model*, Phys. Rev. D **101** (2020) 095024 [arXiv:1812.07592] [INSPIRE].

[117] M. Schmaltz and Y.-M. Zhong, *The leptoquark hunter's guide: large coupling*, JHEP **01** (2019) 132 [arXiv:1810.10017] [INSPIRE].

[118] K. Chandak, T. Mandal and S. Mitra, *Hunting for scalar leptoquarks with boosted tops and light leptons*, Phys. Rev. D **100** (2019) 075019 [arXiv:1907.11194] [INSPIRE].

[119] B.C. Allanach, T. Corbett and M. Madigan, *Sensitivity of future hadron colliders to leptoquark pair production in the di-muon di-jets channel*, Eur. Phys. J. C **80** (2020) 170 [arXiv:1911.04455] [INSPIRE].

[120] L. Buonocore, U. Haisch, P. Nason, F. Tramontano and G. Zanderighi, *Resonant single leptoquark production at hadron colliders*, arXiv:2005.06475 [INSPIRE].

[121] C. Borschensky, B. Fuks, A. Kulesza and D. Schwartländer, *Scalar leptoquark pair production at hadron colliders*, Phys. Rev. D **101** (2020) 115017 [arXiv:2002.08971] [INSPIRE].

[122] M.E. Peskin and T. Takeuchi, *Estimation of oblique electroweak corrections*, Phys. Rev. D **46** (1992) 381 [INSPIRE].

[123] G. Altarelli and R. Barbieri, *Vacuum polarization effects of new physics on electroweak processes*, Phys. Lett. B **253** (1991) 161 [INSPIRE].

[124] I. Doršner, S. Fajfer, A. Greljo, J.F. Kamenik and N. Košnik, *Physics of leptoquarks in precision experiments and at particle colliders*, Phys. Rept. **641** (2016) 1 [arXiv:1603.04993] [INSPIRE].

[125] A. Djouadi, *The anatomy of electro-weak symmetry breaking. II. The Higgs bosons in the minimal supersymmetric model*, Phys. Rept. **459** (2008) 1 [hep-ph/0503173] [INSPIRE].

[126] M. Muhlleitner and M. Spira, *Higgs boson production via gluon fusion: squark loops at NLO QCD*, Nucl. Phys. B **790** (2008) 1 [hep-ph/0612254] [INSPIRE].

[127] R. Bonciani, G. Degrassi and A. Vicini, *Scalar particle contribution to Higgs production via gluon fusion at NLO*, JHEP **11** (2007) 095 [arXiv:0709.4227] [INSPIRE].

[128] M. Carena, I. Low and C.E.M. Wagner, *Implications of a modified Higgs to diphoton decay width*, *JHEP* **08** (2012) 060 [arXiv:1206.1082] [INSPIRE].

[129] W.-F. Chang, J.N. Ng and J.M.S. Wu, *Constraints on new scalars from the LHC* 125 *GeV Higgs signal*, *Phys. Rev. D* **86** (2012) 033003 [arXiv:1206.5047] [INSPIRE].

[130] S. Gori and I. Low, *Precision Higgs measurements: constraints from new oblique corrections*, *JHEP* **09** (2013) 151 [arXiv:1307.0496] [INSPIRE].

[131] C.-S. Chen, C.-Q. Geng, D. Huang and L.-H. Tsai, *New scalar contributions to* $h \to Z\gamma$, *Phys. Rev. D* **87** (2013) 075019 [arXiv:1301.4694] [INSPIRE].

[132] P. Bandyopadhyay and R. Mandal, *Vacuum stability in an extended Standard Model with a leptoquark*, *Phys. Rev. D* **95** (2017) 035007 [arXiv:1609.03561] [INSPIRE].

[133] P. Agrawal and U. Mahanta, *Leptoquark contribution to the Higgs boson production at the CERN LHC collider*, *Phys. Rev. D* **61** (2000) 077701 [hep-ph/9911497] [INSPIRE].

[134] T. Enkhbat, *Scalar leptoquarks and Higgs pair production at the LHC*, *JHEP* **01** (2014) 158 [arXiv:1311.4445] [INSPIRE].

[135] A. Bhaskar, D. Das, B. De and S. Mitra, *Enhancing scalar productions with leptoquarks at the LHC*, *Phys. Rev. D* **102** (2020) 035002 [arXiv:2002.12571] [INSPIRE].

[136] J. Zhang, C.-X. Yue, C.-H. Li and S. Yang, *Constraints on scalar and vector leptoquarks from the LHC Higgs data*, arXiv:1905.04074 [INSPIRE].

[137] V. Gherardi, D. Marzocca and E. Venturini, *Matching scalar leptoquarks to the SMEFT at one loop*, *JHEP* **07** (2020) 225 [arXiv:2003.12525] [INSPIRE].

[138] C.D. Froggatt, R.G. Moorhouse and I.G. Knowles, *Leading radiative corrections in two scalar doublet models*, *Phys. Rev. D* **45** (1992) 2471 [INSPIRE].

[139] E. Keith and E. Ma, *S, T, and leptoquarks at HERA*, *Phys. Rev. Lett.* **79** (1997) 4318 [hep-ph/9707214] [INSPIRE].

[140] H. Abramowicz et al., *The International Linear Collider technical design report — volume* 4*: detectors*, arXiv:1306.6329 [INSPIRE].

[141] M. Aicheler et al., *A multi-TeV linear collider based on CLIC technology: CLIC conceptual design report*, CERN-2012-007, CERN, Geneva, Switzerland (2012) [INSPIRE].

[142] FCC collaboration, *FCC physics opportunities: Future Circular Collider conceptual design report volume* 1, *Eur. Phys. J. C* **79** (2019) 474 [INSPIRE].

[143] FCC collaboration, *FCC-ee: the lepton collider. Future Circular Collider conceptual design report volume* 2, *Eur. Phys. J. ST* **228** (2019) 261 [INSPIRE].

[144] M. Hirsch, H.V. Klapdor-Kleingrothaus and S.G. Kovalenko, *New low-energy leptoquark interactions*, *Phys. Lett. B* **378** (1996) 17 [hep-ph/9602305] [INSPIRE].

[145] V. Gherardi, D. Marzocca and E. Venturini, *Low-energy phenomenology of scalar leptoquarks at one-loop accuracy*, arXiv:2008.09548 [INSPIRE].

[146] M.E. Peskin and T. Takeuchi, *A new constraint on a strongly interacting Higgs sector*, *Phys. Rev. Lett.* **65** (1990) 964 [INSPIRE].

[147] M. Spira, *Higgs boson production and decay at hadron colliders*, *Prog. Part. Nucl. Phys.* **95** (2017) 98 [arXiv:1612.07651] [INSPIRE].

JHEP11(2020)094

[148] J.R. Ellis, M.K. Gaillard and D.V. Nanopoulos, *A phenomenological profile of the Higgs boson*, Nucl. Phys. B **106** (1976) 292 [INSPIRE].

[149] R.N. Cahn, M.S. Chanowitz and N. Fleishon, *Higgs particle production by* $Z \to H\gamma$, Phys. Lett. B **82** (1979) 113 [INSPIRE].

[150] L. Bergstrom and G. Hulth, *Induced Higgs couplings to neutral bosons in* e^+e^- *collisions*, Nucl. Phys. B **259** (1985) 137 [*Erratum ibid.* **276** (1986) 744] [INSPIRE].

[151] T. Inami, T. Kubota and Y. Okada, *Effective gauge theory and the effect of heavy quarks in Higgs boson decays*, Z. Phys. C **18** (1983) 69 [INSPIRE].

[152] A. Djouadi, M. Spira and P.M. Zerwas, *Production of Higgs bosons in proton colliders: QCD corrections*, Phys. Lett. B **264** (1991) 440 [INSPIRE].

[153] M. Spira, A. Djouadi, D. Graudenz and P.M. Zerwas, *Higgs boson production at the LHC*, Nucl. Phys. B **453** (1995) 17 [hep-ph/9504378] [INSPIRE].

[154] ALEPH, DELPHI, L3, OPAL, SLD, LEP Electroweak Working Group, SLD Electroweak Group and SLD Heavy Flavour Group collaborations, *Precision electroweak measurements on the Z resonance*, Phys. Rept. **427** (2006) 257 [hep-ex/0509008] [INSPIRE].

[155] CDF and D0 collaborations, *Combination of CDF and D0 W-boson mass measurements*, Phys. Rev. D **88** (2013) 052018 [arXiv:1307.7627] [INSPIRE].

[156] ATLAS collaboration, *Measurement of* $W^{\pm}$*-boson and Z-boson production cross-sections in pp collisions at* $\sqrt{s} = 2.76$ *TeV with the ATLAS detector*, Eur. Phys. J. C **79** (2019) 901 [arXiv:1907.03567] [INSPIRE].

[157] J. Ellis, C.W. Murphy, V. Sanz and T. You, *Updated global SMEFT fit to Higgs, diboson and electroweak data*, JHEP **06** (2018) 146 [arXiv:1803.03252] [INSPIRE].

[158] J. Bernon and B. Dumont, *Lilith: a tool for constraining new physics from Higgs measurements*, Eur. Phys. J. C **75** (2015) 440 [arXiv:1502.04138] [INSPIRE].

[159] S. Kraml, T.Q. Loc, D.T. Nhung and L.D. Ninh, *Constraining new physics from Higgs measurements with Lilith: update to LHC run 2 results*, SciPost Phys. **7** (2019) 052 [arXiv:1908.03952] [INSPIRE].

[160] F. An et al., *Precision Higgs physics at the CEPC*, Chin. Phys. C **43** (2019) 043002 [arXiv:1810.09037] [INSPIRE].

[161] FCC collaboration, *FCC-hh: the hadron collider. Future Circular Collider conceptual design report volume 3*, Eur. Phys. J. ST **228** (2019) 755 [INSPIRE].

[162] CMS collaboration, *Search for leptoquarks coupled to third-generation quarks in proton-proton collisions at* $\sqrt{s} = 13$ *TeV*, Phys. Rev. Lett. **121** (2018) 241802 [arXiv:1809.05558] [INSPIRE].

[163] ATLAS collaboration, *Searches for scalar leptoquarks and differential cross-section measurements in dilepton-dijet events in proton-proton collisions at a centre-of-mass energy of* $\sqrt{s} = 13$ *TeV with the ATLAS experiment*, Eur. Phys. J. C **79** (2019) 733 [arXiv:1902.00377] [INSPIRE].

[164] ATLAS collaboration, *Searches for third-generation scalar leptoquarks in* $\sqrt{s} = 13$ *TeV pp collisions with the ATLAS detector*, JHEP **06** (2019) 144 [arXiv:1902.08103] [INSPIRE].

JHEP11(2020)094